Regulation by mitochondrial superoxide and NADPH oxidase of cellular formation of nitrated cyclic GMP: potential implications for ROS signaling

Khandaker Ahtesham Ahmed[*], Tomohiro Sawa[*†], Hideshi Ihara[‡], Shingo Kasamatsu[‡], Jun Yoshitake[*], Md. Mizanur Rahaman[*], Tatsuya Okamoto[*], Shigemoto Fujii[*], and Takaaki Akaike[*1]

[*]Department of Microbiology, Graduate School of Medical Sciences, Kumamoto University, 1-1-1 Honjo, Kumamoto 860-8556, Japan, [†]PRESTO, Japan Science and Technology Agency (JST), 4-1-8 Honcho Kawaguchi, Saitama 332-001, Japan, and [‡]Department of Biological Science, Graduate School of Science, Osaka Prefecture University, 1-1 Gakuen-cho, Sakai, Osaka 599-8531, Japan

Running title: ROS-dependent formation of nitrated cyclic GMP

[1]Address correspondence to: Takaaki Akaike, Department of Microbiology, Graduate School of Medical Sciences, Kumamoto University, 1-1-1 Honjo, Kumamoto 860-8556, Japan.
Tel.: +81-96-373-5100; Fax: +81-96-362-8362;
E-mail: takakaik@gpo.kumamoto-u.ac.jp

The abbreviations used are: RNOS, reactive nitrogen oxide species; 8-nitro-cGMP, 8-nitroguanosine 3′,5′-cyclic monophosphate; ROS, reactive oxygen species; MS/MS, tandem mass spectrometry; LPS, lipopolysaccharide; IFN-γ, interferon-γ; TNFα, tumor necrosis factor α; IL-1β, interleukin-1β; Nox, NADPH oxidase; Nox2, NADPH oxidase 2; LC, liquid chromatography; RP, reverse phase; HPLC-ECD, HPLC-electrochemical detection; HPLC-PDA, HPLC-photodiode array with UV detection; ESI, electrospray ionization; siRNA, small interfering RNA; P-NONOate, ($CH_3N[N(O)NO]^-(CH_2)_3NH_2^+CH_3$, 1-hydroxy-2-oxo-3-(*N*-methyl-3-aminopropyl)-3-methyl-1-triazine); SIN-1, 3-morpholinosydnonimine; DTPA, diethylenetriamine- *N*,*N*,*N*',*N*",*N*"-pentaacetic acid; tiron, 1,2-dihydroxy-3,5-benezene-disulfonic acid; MPO, myeloperoxidase; HRP, horseradish peroxidase; SOD, superoxide dismutase; PEG, polyethylene glycol; PEG-SOD, pegylated superoxide dismutase; PEG-catalase, pegylated catalase; DCDHF-DA, 2',7'-dichlorodihydrofluorescein diacetate; mETC, mitochondrial electron-transport chain; sGC, soluble-type guanylyl cyclase; pGC, particulate-type guanylyl cyclases; DHE, dihydroethidium.

8-Nitroguanosine 3′,5′-cyclic monophosphate (8-nitro-cGMP) is a nitrated derivative of cGMP, which can function as a unique electrophilic second messenger involved in regulation of an antioxidant adaptive response in cells. Here, we studied chemical and biochemical regulatory mechanisms involved in 8-nitro-cGMP formation, with particular focus on the roles of reactive oxygen species (ROS). Chemical analyses demonstrated that peroxynitrite-dependent oxidation and myeloperoxidase-dependent oxidation of nitrite in the presence of hydrogen peroxide (H_2O_2) were two major pathways for guanine nucleotide nitration. Among guanine nucleotides examined, GTP was the most sensitive to peroxynitrite-mediated nitration. Immunocytochemical and tandem mass spectrometric analyses revealed that formation of 8-nitro-cGMP in rat C6 glioma cells stimulated with lipopolysaccharide plus proinflammatory cytokines depended on production of both superoxide and H_2O_2. By using the mitochondria-targeted chemical probe MitoSOX Red, we found that mitochondria-derived superoxide can act as a direct determinant of 8-nitro-cGMP formation. Furthermore, we demonstrated that NADPH oxidase 2 (Nox2)-generated H_2O_2 regulated mitochondria-derived superoxide production, which suggests the importance of cross-talk between Nox2-dependent H_2O_2 production and mitochondrial superoxide production. Our data suggest that 8-nitro-cGMP can serve as a unique second messenger that may be implicated in regulating ROS signaling in the presence of nitric oxide.

Key words: Nitric oxide, oxidative stress, reactive oxygen species, mitochondria, ROS signaling, peroxynitrite

INTRODUCTION

cGMP is a cyclic nucleotide formed from GTP by the catalytic action of the enzymes called guanylyl cyclases [1, 2]. In vertebrates, two guanylyl cyclase isoforms have been identified—membrane-bound particulate-type guanylyl cyclase (pGC) and soluble-type guanylyl cyclase (sGC)—that are expressed in almost all cell types [2]. These enzymes are activated in response to specific signals, such as nitric oxide (NO) for sGC and peptide ligands for pGC, to produce cGMP. Subsequently, cGMP functions as a second messenger for these signals and regulates a wide variety of cell physiological functions such as vascular smooth muscle motility, host defense, intestinal fluid and electrolyte homeostasis, and retinal phototransduction [2]. Such biological actions of cGMP may be primarily mediated by activation of downstream effector molecules such as cGMP-dependent protein kinase, ion channels, and phosphodiesterases [2].

Recently, a nitrated derivative of cGMP, 8-nitroguanosine 3′,5′-cyclic monophosphate (8-nitro-cGMP), was identified in mammalian cells [3-6]. 8-Nitro-cGMP possesses unique biochemical properties, e.g., it behaves as an electrophile and reacts with protein sulfhydryls, which results in cGMP adduction to protein sulfhydryls [3, 5, 7, 8]. This post-translational modification by 8-nitro-cGMP via cGMP adduction was named protein *S*-guanylation [3, 5, 7, 8]. Furthermore, 8-nitro-cGMP can induce an antioxidant adaptive response in cells via *S*-guanylation of the redox sensor protein Keap1, which results in transcriptional activation of Nrf2 with concomitant expression of a battery of genes that encode an array of phase II detoxifying or antioxidant enzymes, as well as other cytoprotective proteins [5]. Thus, 8-nitro-cGMP may function as a potent electrophilic second messenger involved in regulation of redox signaling [7-9].

To explore how and when 8-nitro-cGMP is involved in regulating cell physiology via its unique electrophilic property, understanding of the molecular mechanisms regulating 8-nitro-cGMP formation in cells is essential. Nitration of the guanine moiety is a crucial step for production of nitrated nucleotides including 8-nitro-cGMP. Previous studies suggested that reactive nitrogen oxide species (RNOS), formed from the reaction of NO and reactive oxygen species (ROS), can nitrate guanine derivatives under biologically relevant conditions [10, 11]. Examples of RNOS include peroxynitrite ($ONOO^-$), which is a potent oxidizing and nitrating agent formed from the reaction of NO and superoxide (O_2^-). In this study, we investigated the roles of ROS in 8-nitro-cGMP formation both *in vitro* and in cells. Chemical analyses revealed that $ONOO^-$ was a potent agent for nitration of guanine nucleotides. In addition to $ONOO^-$, nitrite in the presence of hydrogen peroxide (H_2O_2) and myeloperoxidase (MPO) may nitrate guanine nucleotides. We used rat C6 glioma cells to study cell formation of 8-nitro-cGMP, because the cells produced a significant amount of 8-nitro-cGMP in response to stimulation with lipopolysaccharide (LPS) plus proinflammatory cytokines via expression of the inducible isoform of NO synthase [5]. In these C6 cells stimulated with LPS-cytokines, mitochondria-derived superoxide acted as a direct determinant of 8-nitro-cGMP formation. This demonstration is the first indicating that mitochondria-derived superoxide plays an important role in biological nitration of guanine nucleotides. Furthermore, we determined that mitochondria-derived superoxide production was regulated by H_2O_2 generated from NADPH oxidase 2 (Nox2), which suggests the importance of cross-talk between Nox2-dependent H_2O_2 production and mitochondrial

superoxide production. Our data thus indicate that 8-nitro-cGMP can serve as a unique second messenger that may be implicated in regulating ROS signaling in the presence of NO.

MATERIALS AND METHODS

Materials

cGMP, GTP, GDP, GMP, and rotenone were obtained from Sigma-Aldrich Corporation, St. Louis, MO. The NO-liberating agent propylamine NONOate ($CH_3N[N(O)NO]^-(CH_2)_3NH_2^+CH_3$, 1-hydroxy-2-oxo-3-(*N*-methyl-3-aminopropyl)-3-methyl-1-triazene) (P-NONOate), which has a half-life of 7.6 min in aqueous solutions at a neutral pH under our experimental conditions, was obtained from Dojindo Laboratories, Kumamoto, Japan. 3-Morpholinosydnonimine (SIN-1), diethylenetriamine- *N*,*N*,*N*′,*N*″,*N*″-pentaacetic acid (DTPA), EDTA, and 1,2-dihydroxy-3,5-benzene-disulfonic acid (tiron) were obtained from Dojindo Laboratories. Tyrosine was obtained from Kyowa Hakko Co. Ltd, Tokyo, Japan. MPO was purchased from Alexis Biochemicals, Plymouth Meeting, PA. Horseradish peroxidase (HRP) was obtained from Wako Pure Chemical Industries, Osaka, Japan. Bovine Cu,Zn-superoxide dismutase (SOD) was purchased from Sigma-Aldrich Corporation. Catalase was purchased from Boehringer Mannheim GmbH, Mannheim, Germany. The succinimidyl derivative of polyethylene glycol (PEG) propionic acid, which has an average molecular mass of M_r 5000, was obtained from NOF Corporation, Tokyo, Japan. NADPH oxidase p47^{phox} small interfering RNA (siRNA) was purchased from Invitrogen, Carlsbad, CA. 2',7'-Dichlorodihydrofluorescein diacetate (DCDHF-DA) and MitoSOX Red, dihydroethidium (DHE), were purchased from Invitrogen Corporation, Molecular Probes, Inc., Eugene, OR. Anti-p47-phox antibody (Catalog no. 07-497) was purchased from Millipore, Temecula, CA. Peroxidase-conjugated anti-mouse secondary antibody was purchased form Amersham Pharmacia Biotech Inc., Piscataway, NJ. For effective delivery of SOD and catalase to the intracellular compartment, those enzymes were chemically modified by conjugation with PEG to obtain the pegylated enzymes (PEG-SOD and PEG-catalase) [12]. SOD (10 mg/ml) or catalase (10 mg/ml) was reacted with succinimidyl PEG (155 mg/ml for SOD and 120 mg/ml for catalase) in 0.5 M sodium phosphate buffer (pH 7.4) for 2 h at 4 ^oC under stirring as previously reported [13]. Authentic $ONOO^-$ was synthesized from acidified nitrite and H_2O_2 by a quenched-flow method according to the literature [14]. The concentration of $ONOO^-$ was determined by means of photospectrometry with a molar absorption coefficient of $\varepsilon_{302} = 1670\ M^{-1}\ cm^{-1}$ [14]. Contaminating H_2O_2 was then decomposed by using manganese dioxide.

Synthesis of various guanine nucleotides

Authentic 8-nitro-cGMP labeled with a stable isotope or unlabeled (8-$^{15}NO_2$-cGMP or 8-$^{14}NO_2$-cGMP, respectively) was prepared according to the method we reported previously [3, 5]. ^{15}N-Labeled cGMP, i.e., [U-$^{15}N_5$, 98%]guanosine 3′,5′-cyclic monophosphate (c[$^{15}N_5$]GMP), was synthesized from [U-$^{15}N_5$, 98%]guanosine 5′-triphosphate ([$^{15}N_5$]GTP; Cambridge Isotope Laboratories, Inc., Andover, MA) via an enzymatic reaction by utilizing purified sGC [5]. All these stable isotope-labeled guanine nucleotides were used as internal standards in the stable isotope dilution technique with liquid chromatography (LC)-tandem mass spectrometry (MS/MS) analysis, as described below. Authentic

8-nitro-GMP, 8-nitro-GDP, and 8-nitro-GTP were prepared by reacting 1 mM GMP, GDP, and GTP, respectively, with 2 mM $ONOO^-$ in 0.1 M sodium phosphate buffer (pH 7.4) containing 25 mM $NaHCO_3$ and 0.1 mM DTPA.

Chemical analysis of guanine nucleotide nitration in vitro

Guanine nucleotides were reacted with various RNOS systems *in vitro* to determine the nitrating potential of each RNOS system. Formation of nitrated derivatives was analyzed by means of reverse-phase (RP)-HPLC equipped with a photodiode array (PDA) or with electrochemical detection (ECD) [3]. RP-HPLC-ECD was used for analysis of cGMP nitration, whereas RP-HPLC-PDA was used for analysis of nitration of other guanine nucleotides. For RP-HPLC-PDA, HPLC plus PDA detection was performed with a UV detector using an MCM C-18 column (150 mm long, 4.6 mm inner diameter; MC Medical, Inc., Tokyo, Japan). Samples were eluted with 0-40% CH_3CN in 1.0% dibutylammonium acetate buffer with a 0.7 ml/min flow rate; detection was by HPLC-PDA, with a UV detector (SPD-M10A VP; Shimadzu, Kyoto, Japan).

Authentic $ONOO^-$ system

The guanine nucleotides cGMP, GMP, GDP, and GTP (each at 1 mM) were reacted under vortex mixing with authentic $ONOO^-$ (2 mM) in 0.1 M sodium phosphate buffer (pH 7.4) containing 25 mM $NaHCO_3$ and 0.1 mM DTPA. Nitration of cGMP by $ONOO^-$ was further analyzed as a function of $ONOO^-$ concentration and buffer pH. That is, cGMP (50 µM) was reacted under vortex mixing with $ONOO^-$ (up to 10 µM) in 0.1 M sodium phosphate buffer (pH 7.4) containing 0.1 mM DTPA with or without 25 mM $NaHCO_3$. The effect of pH was examined for the pH range of 2.5-7.4. Buffers used included 0.1 M citric acid buffer (pH 2.5-5.0) and 0.1 M sodium phosphate buffer (pH 5.5-7.4), containing 0.1 mM DTPA with or without 25 mM $NaHCO_3$.

SIN-1 system

SIN-1 was used to study the effect of simultaneous production of NO and superoxide [15] on guanine nucleotide nitration. cGMP (50 µM) or tyrosine (50 µM) was reacted with SIN-1 (0-100 µM) in 0.1 M sodium phosphate buffer (pH 7.4) in the presence of 0.1 mM DTPA and 25 mM $NaHCO_3$.

Nitrite/H_2O_2/heme peroxidase system

Heme peroxidases catalyze oxidation of nitrite in the presence of H_2O_2 to form the potent nitrating agent nitrogen dioxide (NO_2) [16, 17]. In our study here, two heme peroxidases—MPO and HRP—were used as catalysts. cGMP (50 µM) or tyrosine (50 µM) was reacted at 37 °C for 3 h with either MPO (10 nM) or HRP (23.8 nM) in 0.1 M sodium phosphate buffer (pH 7.4) containing 100 µM $NaNO_2$ and 100 µM H_2O_2.

Aerobic NO production system

NO is oxidized to form NO_2, an oxidizing and nitrating agent, under aerobic conditions [18]. To study the effect of NO and NO_2 on guanine nucleotide nitration, we used the NO-releasing agent

P-NONOate, which spontaneously decomposes to release NO [19]. cGMP (50 μM) and tyrosine (50 μM) were reacted with P-NONOate (0-100 μM), an NO donor in 0.1 M sodium phosphate buffer (pH 7.4), in the presence of 0.1 mM DTPA and 25 mM $NaHCO_3$, followed by measurement of the nitrated derivatives of cGMP and tyrosine. Nitration of cGMP and tyrosine was also examined in an acidified nitrite system [18]: cGMP (50 μM) and tyrosine (50 μM) were reacted for 1 h at 37 °C with $NaNO_2$ (100 μM) in 0.1 M sodium citrate buffer (pH 2.5-4.5).

Hypochlorous acid/nitrite system

Hypochlorous acid (HOCl) is a product of the MPO-catalyzed oxidation of chlorine ion (Cl^-) in the presence of H_2O_2. HOCl reportedly reacts with nitrite to form NO_2Cl [20]. To determine the effect of NO_2Cl on guanine nucleotide nitration, cGMP (50 μM) and tyrosine (50 μM) were reacted for 4 h at 37 °C with HOCl (100 μM) plus $NaNO_2$ (100 μM) in 0.1 M sodium phosphate buffer (pH 7.4).

Effects of ROS scavengers

To determine the roles of ROS on guanine nucleotide nitration, we used three different ROS scavengers: SOD and tiron for scavenging superoxide and catalase for scavenging H_2O_2. For the experiments described below, pegylated SOD and catalase were used for effective delivery of those enzymes into cells [12].

Cell treatment

Rat C6 glioma cells were cultured at 37 °C in Dulbecco's modified Eagle's medium (Wako Pure Chemical Industries) supplemented with 10% fetal bovine serum and 1% penicillin-streptomycin. Cells were plated at a density of 1.5×10^6 cells per 60-mm dish to prepare cell extracts for LC-electrospray ionization-MS/MS (LC-ESI-MS/MS), and at a density of 1×10^5 cells per chamber in BD Falcon Culture Slides (BD Biosciences, San Jose, CA) for immunocytochemistry. To study 8-nitro-cGMP formation, cells were stimulated for 36 h with a mixture of 10 μg/ml LPS (from *Escherichia coli*; L8274; Sigma-Aldrich Corporation) and 200 U/ml interferon-γ (IFN-γ), 500 U/ml tumor necrosis factor α (TNFα), and 10 ng/ml interleukin-1β (IL-1β) (all cytokines from R&D Systems, Inc., Minneapolis, MN). In some experiments, to investigate the mechanism of ROS-dependent 8-nitro-cGMP production, cells were stimulated in the presence of ROS scavengers, including PEG-SOD, tiron, and PEG-catalase, followed by analyses for 8-nitro-cGMP formation and ROS generation. In certain experiments, cells were treated with an LPS-cytokine mixture for 0, 3, 12, 24, and 36 h followed by detection of mitochondrial ROS by MitoSOX Red, as described below. In other experiments to investigate involvement of mitochondrial ROS generation in 8-nitro-cGMP formation, cells were pretreated for 15 min with 10 μM rotenone before LPS-cytokine stimulation. To study the role of Nox2 in cellular ROS production, cells were transfected with NADPH oxidase $p47^{phox}$-specific siRNA before stimulation as described below.

Immunocytochemistry

Formation of 8-nitro-cGMP in C6 cells was analyzed by means of immunocytochemistry with

anti-8-nitro-cGMP mouse monoclonal antibody and Cy3-labeled goat anti-mouse IgG antibody (PA43002, 10 µg/ml; Amersham Biosciences Corporation, Piscataway, NJ), as described previously [3, 5]. Fluorescence intensity values from three different experiments were obtained, and the average relative fluorescence intensity (as percent fluorescence intensity) was determined for LPS-cytokine-stimulated cells. We confirmed that LPS-cytokines and PEG-derivatized proteins had no significant effects on quenching or augmentation of fluorescence by using nonimmune antiserum (data not shown).

LC-ESI-MS/MS analysis for intracellular formation of 8-nitro-cGMP

Intracellular levels of 8-nitro-cGMP were quantified by means of LC-ESI-MS/MS as described previously [5]. Amounts of endogenous cGMP and 8-nitro-cGMP were determined via the stable isotope dilution method based on the recovery efficiency of stable isotope-labeled derivatives (c[$^{15}N_5$]GMP and 8-$^{15}NO_2$-cGMP) spiked with the cell extract as described previously [5].

Determination of cellular ROS production

Cellular ROS production was determined by means of fluorescence microspectrometry with chemical probes that become fluorescent on reaction with ROS. Specifically, we used MitoSOX Red [21] and DHE [22] for detection of mitochondrial superoxide production and DCDHF-DA [23] for detection of cellular oxidants. C6 cells were washed with Hank's buffer, pH 7.4 (0.137 M NaCl, 5.4 mM KCl, 0.25 mM Na_2HPO_4, 0.44 mM KH_2PO_4, 1.3 mM $CaCl_2$, 1.0 mM $MgSO_4$, 4.2 mM $NaHCO_3$), and were then stained with 2.5 µM MitoSOX Red or with 100 nM DHE dissolved in Hank's buffer, or with 5 µM DCDHF-DA dissolved in PBS, for 15 min at 37 °C in the dark. Cells were then washed carefully with Hank's buffer, mounted with mounting buffer, covered with coverslips, and examined with a Nikon EZ-C1 confocal laser microscope. Excitation was at 420 nm for MitoSOX Red and 543 nm for DHE (the red photomultiplier channel of the confocal microscope was used for image acquisition); for DCDHF-DA, excitation was at 488 nm (the green photomultiplier channel of the confocal microscope was used for image acquisition). To minimize run-to-run variations, the laser intensity and photomultiplier tube voltage were kept constant, and microscopic observations were performed on all sample sets at same time. Images were captured and processed by means of Nikon EZ-C1 software. Further image processing and quantification were performed by using Adobe Photoshop Elements v. 2.0 (Adobe Systems). Fluorescence intensity values from three different experiments were obtained, and the average relative fluorescence intensity (as percent fluorescence intensity) was determined for LPS-cytokine-stimulated cells. In other experiments, the percent relative fluorescence intensity was determined for PBS-treated cells.

Transfection of p47^{phox} siRNA

A 25-nucleotide p47^{phox} siRNA (Catalog no. 1320003, Oligo ID, MSS206956 and MSS275934; manufactured by Invitrogen) was used for transfection using the Lipofectamine RNAiMAX transfection reagent (Invitrogen). Briefly, C6 cells were seeded in 12-well plates at a density of 2 × 10^5 cells/well. Cells were transfected with p47^{phox} siRNA (60 pmol/well) by using Lipofectamine

RNAiMAX transfection reagent. At 72 h after transfection, cells were harvested, but just before the harvest they were treated with LPS-cytokines for 36 h. Stealth RNAi negative control (high GC; Invitrogen) was used as a negative control siRNA as described above. In other experiments, cells were treated with 10 μM rotenone for 15 min before stimulation with LPS-cytokines for 36 h.

Western blot analysis

Proteins were separated by using SDS-PAGE and transferred onto a PVDF membrane. The blot was blocked with 5% skim milk followed by 1 h of incubation with anti-p47-phox antibody (Millipore, Temecula, CA) and a goat anti-rabbit HRP-conjugated IgG secondary antibody. The immunoreactive bands were detected by using a chemiluminescence reagent (Millipore, Bedford, MA) with a luminescent image analyzer (LAS-1000; Fujifilm, Tokyo, Japan).

Statistical analysis

All cell culture data were obtained from at least 3 separate wells or 3 separate dishes, and the data are represented as means ± S.E. Statistical analyses were performed by using Student's *t* test.

RESULTS

Nitration of guanine nucleotides by various RNOS: in vitro chemical analyses

We investigated the effects of various RNOS on nitration of guanine nucleotides *in vitro*. We first examined nitration of guanine nucleotides in the reaction with $ONOO^-$, a potent nitrating and oxidizing species formed from the reaction of NO and superoxide. As Fig. 1*A* shows, $ONOO^-$ nitrated all guanine nucleotides. However, the efficacy of nitration varied depending on the structure of the nucleotides; GTP evidenced the highest production of nitrated derivative, with nitration efficiency then decreasing in the following order: GDP > GMP > cGMP.

Nitration of guanine nucleotides by $ONOO^-$ was further examined as a function of $ONOO^-$ concentration and pH of the reaction mixtures, with cGMP used as a model substrate. As illustrated in Fig. 1*B*, formation of 8-nitro-cGMP depended on the concentration of $ONOO^-$. 8-Nitro-cGMP formation was markedly enhanced in the presence of $NaHCO_3$. This enhanced effect of $NaHCO_3$ on $ONOO^-$-mediated nitration was more obvious for cGMP than for tyrosine. The efficacies of $ONOO^-$-mediated nitration of both cGMP and tyrosine were maximum at neutral pH (pH 7-7.2) (Fig. 1*C*). To exclude the possibility that nitrite that may be contaminating the $ONOO^-$ solution could affect the induction of cGMP nitration, we examined cGMP nitration in a reaction with decomposed $ONOO^-$ solution that would presumably contain the same amount of contaminating nitrite as an intact $ONOO^-$ solution. Results indicated no 8-nitro-cGMP formation in the reaction of cGMP with decomposed $ONOO^-$ (data not shown).

Table 1 summarizes the effects of various RNOS systems on nitration of cGMP and tyrosine. The NO donor P-NONOate did not cause detectable nitration of cGMP even under aerobic conditions. An acidic nitrite system did cause tyrosine nitration but no detectable formation of 8-nitro-cGMP. SIN-1, which simultaneously generates NO and superoxide, caused both cGMP and tyrosine nitration. This result suggests that $ONOO^-$ formed from NO and superoxide is an effective nitrating agent for guanine

nucleotides. In addition to SIN-1, the complete $NaNO_2/H_2O_2$/MPO system led to marked nitration of cGMP. Omission of just one component from this complete system resulted in no detectable level of 8-nitro-cGMP. HOCl is a strong oxidant produced by MPO. $NaNO_2$ in the presence of HOCl effectively nitrated tyrosine but not cGMP. No 8-nitro-cGMP formed after replacement of MPO by HRP in the complete system, which suggests that nitration of guanine nucleotides depends on the type of peroxidase even when both nitrite anion and H_2O_2 are available simultaneously.

Nitration of cGMP by RNOS was inhibited by specific inhibitors and scavengers of ROS (Fig. 2). SOD completely suppressed SIN-1-mediated cGMP nitration, whereas it failed to suppress nitration of cGMP mediated by authentic $ONOO^-$ or $NaNO_2/H_2O_2$/MPO. Catalase, however, was an effective inhibitor of only $NaNO_2/H_2O_2$/MPO-mediated nitration of cGMP. Tiron is a small molecule that is an SOD mimic and has been used as a superoxide scavenger [24]. In our study here, however, tiron effectively suppressed cGMP nitration mediated by all RNOS systems examined. Similarly, tiron effectively suppressed tyrosine nitration caused by authentic $ONOO^-$ (supplemental Fig. S1). It was also found that tiron effectively suppressed tyrosine nitration by P-NONOate, suggesting that tiron can inhibit nitration by either $ONOO^-$ or aerobic NO (NO_2) possibly via scavenging NO_2, independent of its superoxide scavenging activity.

Formation of 8-nitro-cGMP in rat C6 glioma cells: involvement of cellular ROS production

Our chemical analyses clearly demonstrated that NO itself is not sufficient to cause nitration of guanine nucleotides but requires ROS including superoxide and H_2O_2 for that reaction to occur. To study the roles of ROS in 8-nitro-cGMP formation in cells, we used C6 cells in culture as a model system.

Immunocytochemical analyses provided the baseline formation of 8-nitro-cGMP in nonstimulated C6 cells (Fig. 3*A*). Formation of 8-nitro-cGMP was markedly enhanced in C6 cells when cells were stimulated with LPS-cytokines (Fig. 3*A*). Treatment with PEG-SOD, which is reportedly a membrane-permeable SOD derivative [12], reduced the immunostaining in a manner dependent on PEG-SOD concentration (Fig. 3*B*). This result suggests the essential role of superoxide for cell formation of 8-nitro-cGMP in stimulated C6 cells. Similar to PEG-SOD, PEG-catalase, a membrane-permeable catalase derivative, suppressed 8-nitro-cGMP formation in C6 cells stimulated with LPS-cytokines (Fig. 3*C*). LC-ESI-MS/MS analyses verified 8-nitro-cGMP formation in C6 cells and its modulation by PEG-SOD and PEG-catalase. In agreement with immunocytochemical data, these analyses detected a certain level of 8-nitro-cGMP in nonstimulated C6 cells (Fig. 4). As Fig. 4 shows, stimulation by LPS-cytokines significantly promoted formation of both cGMP and 8-nitro-cGMP in C6 cells. The concentration of 8-nitro-cGMP was about 5.6 times higher than that of cGMP under current experimental conditions. PEG-SOD treatment moderately reduced the level of cGMP. A similar trend was observed with PEG-catalase, although it was not statistically significant. Formation of 8-nitro-cGMP was almost completely nullified by treatment with both PEG-SOD and PEG-catalase, a finding that agrees with results obtained by immunocytochemistry. Thus, these data suggest that formation of 8-nitro-cGMP depends greatly on cell production of both superoxide and H_2O_2. Under these condition, PEG-SOD and PEG-catalase treatments did not affect NO production in

C6 cells (supplemental Fig. S2).

Cellular production of ROS and related oxidants was analyzed by using chemical probes that become fluorescent in response to ROS and oxidants. With MitoSOX Red, a mitochondria-targeted superoxide-sensitive fluorogenic probe [21], we found that stimulation of C6 cells with LPS-cytokines significantly induced production of mitochondrial superoxide (Fig. 5*A*). A time course study showed that mitochondrial superoxide production gradually increased and reached a plateau at 24 h after LPS-cytokine stimulation (supplemental Fig. S3). On the basis of this result, analyses of ROS production were carried out at 36 h after stimulation. We also used double staining of cells with MitoTracker Green and MitoSOX Red to investigate whether the MitoSOX Red signal was derived from mitochondria. As supplemental Fig. S4 shows, MitoSOX Red staining co-localized well with MitoTracker Green staining, which suggests that the superoxide detected by MitoSOX Red was primarily of mitochondrial origin.

Treatment with PEG-SOD significantly reduced the fluorescence intensity originating with MitoSOX Red (Fig. 5*B*). PEG-catalase also suppressed production of superoxide, as shown by reduced MitoSOX Red-derived fluorescence. These results suggest that mitochondrial superoxide production may be regulated by H_2O_2 production. We then studied production of H_2O_2 by using DCDHF-DA, a cell-permeable and oxidation-sensitive fluorescent probe. Microscopic observation of DCDHF-DA-derived fluorescence clearly showed oxidant production in C6 cells after stimulation with LPS-cytokines (Fig. 5*A*). A significant inhibitory effect of PEG-catalase (Fig. 5*B*) suggests that H_2O_2 is produced in stimulated C6 cells and acts as a major oxidant involved in induction of DCDHF-derived fluorescence. The specificity of superoxide detection was confirmed by using DHE, and the results were consistent with those obtained by MitoSOX Red analysis (Fig. 5).

As mentioned above, tiron can act not only as a superoxide scavenger but also as an antioxidant to inhibit guanine nucleotide nitration caused by $ONOO^-$ and $NaNO_2/H_2O_2$/MPO (Fig. 2). Immunocytochemical analyses revealed that tiron effectively suppressed formation of 8-nitro-cGMP in C6 cells stimulated with LPS-cytokines (Fig. 6). Similarly, tiron treatment significantly reduced fluorescence derived from both MitoSOX Red and DCDHF (Fig. 6). Under these conditions, tiron did not cause any detectable cytotoxic effects (supplemental Fig. S5).

Mitochondrial electron-transport chain (mETC) complexes, particularly complexes I and III, are the main source of ROS produced from mitochondria [25]. The mETC inhibitor rotenone reportedly accelerates or inhibits mitochondrial ROS production dependent on the cell type studied [26, 27]. We thus studied whether modulation of mitochondrial ROS production with the mETC complex inhibitor rotenone affected formation of 8-nitro-cGMP in C6 cells. As Fig. 7 shows, rotenone treatment increased 8-nitro-cGMP formation in C6 cells stimulated with LPS-cytokines, as evidenced by immunocytochemistry and LC-ESI-MS/MS results: both methods revealed a similar increase, by approximately 1.5 fold. Under the same experimental conditions, rotenone treatment significantly increased MitoSOX Red-derived fluorescence intensity without affecting DCDHF-derived fluorescence (Fig. 7*B*). This finding suggests that the effect of rotenone was specific to mitochondrial ROS production and hence that 8-nitro-cGMP formation in C6 cells is closely related to mitochondrial superoxide production. However, treatment of nonstimulated cells with rotenone alone did not

significantly affect the production of 8-nitro-cGMP, and, in fact, an increased MitoSOX Red signal was observed (Fig. 7). This result suggests that 8-nitro-cGMP production requires simultaneous production of both NO and ROS.

Nox2 is a member of the NADPH oxidase family and is an important source of ROS, particularly in immunologically stimulated cells [28]. To clarify the implications of Nox2-dependent ROS production for 8-nitro-cGMP formation, we performed knockdown of $p47^{phox}$, a critical component of Nox, by using $p47^{phox}$ siRNA. The efficacy of the $p47^{phox}$ knockdown was confirmed by Western blotting (Fig. 8). In C6 cells treated with $p47^{phox}$ siRNA, immunocytochemistry revealed marked suppression of 8-nitro-cGMP formation (Fig. 8). The $p47^{phox}$ knockdown also significantly suppressed production of mitochondrial superoxide and cellular oxidant as determined by fluorescence microscopy (Fig. 8). As shown in supplemental Fig.S6, superoxide and H_2O_2 productions were remarkably augmented by LPS-cytokines stimulation and suppressed by $p47^{phox}$ siRNA treatment. Levels of H_2O_2 were approximately 5 times lower than those of superoxide. This may be due, at least in part, by differences of methods used. Superoxide was captured by cytochrome c in situ when generated extracellularly. On the other hand, concentrations of H_2O_2 were determined after 10 min accumulation in culture supernatant. During 10 min incubation, some part of H_2O_2 produced extracellularly would be consumed by cells so that values determined for H_2O_2 accumulation reflected to the differences between the production and consumption.

We also performed investigations to see whether mitochondria could produce ROS under a $p47^{phox}$ knockdown condition. As seen in supplemental Fig. S7, we found that rotenone treatment along with LPS-cytokines in Nox2 knockdown cells increased mitochondrial superoxide production independent of the Nox2-generated ROS. This finding suggests that even though the mitochondrial respiratory chain is intact in Nox2 knockdown cells, its superoxide production is impaired under the current stimulation conditions. All these results together suggest that Nox2 contributes to the formation of 8-nitro-cGMP via production of H_2O_2, which in turn enhances mitochondrial superoxide production.

To study the role of H_2O_2 in formation of 8-nitro-cGMP and its association with mitochondrial superoxide production, we treated C6 cells with NO donors and H_2O_2. P-NONOate alone had a negligible effect on 8-nitro-cGMP formation (Fig. 9*A* and supplemental Fig. S8*A*). Treatment with H_2O_2 slightly increased 8-nitro-cGMP formation, and PEG-SOD treatment suppressed this increment. 8-Nitro-cGMP formation significantly increased in C6 cells that were simultaneously treated with both P-NONOate and H_2O_2. Furthermore, PEG-SOD treatment markedly suppressed 8-nitro-cGMP formation induced by P-NONOate plus H_2O_2. To clarify whether extracellular H_2O_2 can directly accelerate mitochondrial superoxide production, we examined the effect of H_2O_2 treatment on MitoSOX Red fluorescence. In fact, we found that H_2O_2 treatment significantly increased mitochondrial superoxide production (Fig. 9*B* and supplemental Fig. S8*B*). Taken together, in stimulated C6 cells, H_2O_2 derived from Nox2 may play a role in NO-dependent formation of 8-nitro-cGMP, possibly via accelerating superoxide production in mitochondria.

DISCUSSION

In this study, we investigated the chemical and biochemical mechanisms of 8-nitro-cGMP formation,

with particular focus on the roles of ROS. Our chemical analyses showed that NO itself is not sufficient to nitrate guanine nucleotides *in vitro*. Two reaction systems, $ONOO^-$ and $NaNO_2/H_2O_2/MPO$, effectively produced nitrated guanine nucleotides. At physiological pH, both $ONOO^-$ and its conjugated acid ONOOH (pK_a = 6.8) exist, and the latter decomposes via homolysis to give the hydroxyl radical ($^{\bullet}OH$) and NO_2 [29]. In the presence of CO_2, $ONOO^-$ reacts with CO_2 to form nitrosoperoxycarbonate anion ($ONOOCO_2^-$), which undergoes homolysis to give $CO_3^{\bullet-}$ and NO_2 [30]. Reduction potentials have been reported for $^{\bullet}OH$ (E^0 = 1.9-2.1 V) [31], NO_2 (E^0 = 1.04 V) [32], $CO_3^{\bullet-}$ (E^0 = 1.5 V) [33], and guanine (E^0 = 1.29 V) [34]. Oxidation of guanine by $^{\bullet}OH$ or $CO_3^{\bullet-}$ is thus believed to be thermodynamically favorable and would result in formation of the guanine radical cation. This cation undergoes recombination with NO_2 to form 8-nitroguanine [11]. A similar mechanism may therefore operate for nitration of guanine nucleotides induced by $ONOO^-$ and $ONOOCO_2^-$. The $NaNO_2/H_2O_2/MPO$ system used in this study was another potent mechanism for nitration of guanine nucleotides. MPO reacts with H_2O_2 to form MPO compound I, which can oxidize nitrite and produce NO_2 [35]. This compound I may also directly oxidize guanine nucleotides because of its strong reduction potential (E^0 = 1.35 V) [36]. In contrast, we found no production of nitrated guanine nucleotides in the reaction of guanine nucleotides with $NaNO_2/H_2O_2$/HRP. HRP compound I is reportedly a much weaker one-electron oxidant compared with MPO compound I [37]. Therefore, HRP compound I could not oxidize guanine nucleotides to form the corresponding cation radical.

We determined that GTP, among the guanine nucleotides examined, was the most susceptible to nitration induced by $ONOO^-$. GTP makes up nearly 25% of the total intracellular nucleotide triphosphate pool, and it acts as a versatile nucleotide, as it participates in many critical physiological functions including RNA synthesis, cell signaling through activation of GTP-binding proteins, and production of the second messenger cGMP [38]. Electrophilic activity of nitrated guanine nucleotides varies dependent on their structures (unpublished data). Among 8-nitroguanine derivatives examined, 8-nitro-cGMP showed the highest electrophilic activity at neutral pH, and the electrophilic activity decreasing in the following order: 8-nitro-cGMP >> 8-nitroguanosine > 8-nitro-GTP, 8-nitro-GMP. The second-order rate constants for the reaction of glutathione with those molecules were determined to be 0.05 (8-nitro-cGMP), 0.018 (8-nitroguanosine), 0.01 (8-nitro-GTP), and 0.008 (8-nitro-GMP) $M^{-1}s^{-1}$, respectively [3, unpublished result]. In this context, 8-nitro-GTP may stably be present in cytosol where glutathione is present abundantly. On the other hand, our previous work demonstrated that 8-nitro-GTP can act as a substrate for sGC, with 8-nitro-cGMP formed as a product [5]. These data suggest that 8-nitro-GTP may implicate in electrophile signaling via acting as an excellent substrate for guanylate cyclase to produce 8-nitro-cGMP, rather than inducing direct protein *S*-guanylation.

Although $ONOO^-$ has been considered as toxic byproduct of NO and ROS formation, accumulating evidence points its signaling function. Kang et al. reported that $ONOO^-$ formed under sulfur amino acid deprivation activates Nrf2 signal via the pathway of phosphatidylinositol 3-kinase (PI3K) [39]. Our previous study revealed that Nrf2 signal can be activated, at least in part, via Keap1 *S*-guanylation, as supported by the fact that reduction of 8-nitro-cGMP formation by sGC inhibitor appreciably suppressed Nrf2 nuclear translocation and heme oxygenase-1 gene expression, without affecting

RNOS formation [5]. It is thus speculated that $ONOO^-$ may contribute to activation of Nrf2-dependent responses via multiple mechanisms including increased production of electrophilic molecules such as 8-nitro-cGMP and activation of PI3K pathway.

Our present study showed that Nox2 and mitochondria are two important sources of ROS in rat C6 glioma cells stimulated by LPS-cytokines and are critically involved in regulation of 8-nitro-cGMP formation. The levels of H_2O_2 from stimulated C6 cells were determined to be 1.63 ± 0.03 nmol/min/mg protein (or 3.0 ± 0.2 μM in culture supernatant for 10 min incubation under the current condition). In our separate experiments, 10 μM of H_2O_2 added exogenously to non-stimulated cells sufficiently induced mitochondrial superoxide production and 8-nitro-cGMP formation in the presence of NO donor (Supplemental Fig. S8). These observations suggest that ~10 μM H_2O_2 is required to promote mitochondrial superoxide production in C6 cells. Recent studies have suggested superoxide production in mitochondria is accelerated by H_2O_2 [40]. We therefore speculate that H_2O_2 derived from Nox2 contribute to the acceleration of mitochondrial superoxide generation, and hence, 8-nitro-cGMP formation as illustrated in Fig. 10. In this context, recent study by Zhang et al demonstrating local production of superoxide by Nox4 in sarcoplasmic reticulum [41], suggesting that regulation of ROS signaling by different Nox enzymes in certain cell types, and warrants further investigation of 8-nitro-cGMP signaling in these cells.

In summary, we herein verified that ROS play a pivotal role in the formation of 8-nitro-cGMP in C6 cells stimulated with LPS-cytokines. Superoxide, most likely derived from mitochondria, is directly involved in formation of 8-nitro-cGMP, whereas H_2O_2 generated by Nox2 also has an important role by increasing mitochondrial superoxide production. Our data thus suggest that 8-nitro-cGMP may serve as a unique second messenger for ROS signaling in the presence of NO. Greater understanding of 8-nitro-cGMP formation in relation to mitochondrial functions and NADPH oxidase regulation may help us develop new diagnostic methods and treatment of diseases related to dysregulation of NO and ROS [42].

AUTHOR CONTRIBUTION

Khandaker Ahtesham Ahmed and Tomohiro Sawa designed and performed experiments, analyzed data and wrote the paper. Hideshi Ihara, Shingo Kasamatsu, and Jun Yoshitake contributed to acquisition of LC-MS/MS data. Tatsuya Okamoto, Md. Mizanur Rahaman and Shigemoto Fujii performed immunocytochemistry, cytotoxicity assays, superoxide and H_2O_2 measurements and Western blotting experiments. Takaaki Akaike designed and supervised the project, and wrote the paper. All authors read and approved the final version of the manuscript.

ACKNOWLEDGEMENTS

We thank Judith B. Gandy for excellent editing of the manuscript.

FUNDING

This work was supported in part by Grants-in-Aid for Scientific Research [grant number 21390097 and 21590312] and Grants-in-Aid for Scientific Research on Innovative Areas (Research in a

Proposed Area) [grant number 20117001 and 20117005] from the Ministry of Education, Sciences, Sports and Technology (MEXT), Japan, and JST PRESTO program [grant number 09801194].

REFERENCES

1. Murad, F. (1986) Cyclic guanosine monophosphate as a mediator of vasodilation. J. Clin. Invest. **78**, 1-5
2. Lucas, K. A., Pitari, G. M., Kazerounian, S., Ruiz-Stewart, I., Park, J., Schulz, S., Chepenik, K. P. and Waldman, S. A. (2000) Guanylyl cyclases and signaling by cyclic GMP. Pharmacol. Rev. **52**, 375-414
3. Sawa, T., Zaki, M. H., Okamoto, T., Akuta, T., Tokutomi, Y., Kim-Mitsuyama, S., Ihara, H., Kobayashi, A., Yamamoto, M., Fujii, S., Arimoto, H. and Akaike, T. (2007) Protein S-guanylation by the biological signal 8-nitroguanosine 3',5'-cyclic monophosphate. Nat. Chem. Biol. **3**, 727-735
4. Zaki, M. H., Fujii, S., Okamoto, T., Islam, S., Khan, S., Ahmed, K. A., Sawa, T. and Akaike, T. (2009) Cytoprotective function of heme oxygenase 1 induced by a nitrated cyclic nucleotide formed during murine salmonellosis. J. Immunol. **182**, 3746-3756
5. Fujii, S., Sawa, T., Ihara, H., Tong, K. I., Ida, T., Okamoto, T., Ahtesham, A. K., Ishima, Y., Motohashi, H., Yamamoto, M. and Akaike, T. (2010) The critical role of nitric oxide signaling, via protein S-guanylation and nitrated cyclic GMP, in the antioxidant adaptive response. J. Biol. Chem. **285**, 23970-23984
6. Ihara, H., Ahmed, K. A., Ida, T., Kasamatsu, S., Kunieda, K., Okamoto, T., Sawa, T. and Akaike, T. (2011) Methodological proof of immunocytochemistry for specific identification of 8-nitroguanosine 3',5'-cyclic monophosphate formed in glia cells. Nitric Oxide **25**, 169-175
7. Akaike, T., Fujii, S., Sawa, T. and Ihara, H. (2010) Cell signaling mediated by nitrated cyclic guanine nucleotide. Nitric Oxide **23**, 166-174
8. Ahmed, K. A., Sawa, T. and Akaike, T. (2011) Protein cysteine S-guanylation and electrophilic signal transduction by endogenous nitro-nucleotides. Amino Acids **41**, 123-130
9. Feelisch, M. (2007) Nitrated cyclic GMP as a new cellular signal. Nat. Chem. Biol. **3**, 687-688
10. Sawa, T. and Ohshima, H. (2006) Nitrative DNA damage in inflammation and its possible role in carcinogenesis. Nitric Oxide **14**, 91-100
11. Niles, J. C., Wishnok, J. S. and Tannenbaum, S. R. (2006) Peroxynitrite-induced oxidation and nitration products of guanine and 8-oxoguanine: structures and mechanisms of product formation. Nitric Oxide **14**, 109-121
12. Beckman, J. S., Minor, R. L., Jr., White, C. W., Repine, J. E., Rosen, G. M. and Freeman, B. A. (1988) Superoxide dismutase and catalase conjugated to polyethylene glycol increases endothelial enzyme activity and oxidant resistance. J. Biol. Chem. **263**, 6884-6892
13. Sawa, T., Wu, J., Akaike, T. and Maeda, H. (2000) Tumor-targeting chemotherapy by a xanthine oxidase-polymer conjugate that generates oxygen-free radicals in tumor tissue. Cancer Res. **60**, 666-671

14. Koppenol, W. H., Kissner, R. and Beckman, J. S. (1996) Syntheses of peroxynitrite: to go with the flow or on solid grounds? Methods Enzymol. **269**, 296-302
15. Darley-Usmar, V. M., Hogg, N., O'Leary, V. J., Wilson, M. T. and Moncada, S. (1992) The simultaneous generation of superoxide and nitric oxide can initiate lipid peroxidation in human low density lipoprotein. Free Radic. Res. Commun. **17**, 9-20
16. van der Vliet, A., Eiserich, J. P., Halliwell, B. and Cross, C. E. (1997) Formation of reactive nitrogen species during peroxidase-catalyzed oxidation of nitrite. A potential additional mechanism of nitric oxide-dependent toxicity. J. Biol. Chem. **272**, 7617-7625
17. Eiserich, J. P., Hristova, M., Cross, C. E., Jones, A. D., Freeman, B. A., Halliwell, B. and van der Vliet, A. (1998) Formation of nitric oxide-derived inflammatory oxidants by myeloperoxidase in neutrophils. Nature **391**, 393-397
18. O'Donnell, V. B., Eiserich, J. P., Chumley, P. H., Jablonsky, M. J., Krishna, N. R., Kirk, M., Barnes, S., Darley-Usmar, V. M. and Freeman, B. A. (1999) Nitration of unsaturated fatty acids by nitric oxide-derived reactive nitrogen species peroxynitrite, nitrous acid, nitrogen dioxide, and nitronium ion. Chem. Res. Toxicol. **12**, 83-92
19. Sawa, T., Akaike, T. and Maeda, H. (2000) Tyrosine nitration by peroxynitrite formed from nitric oxide and superoxide generated by xanthine oxidase. J. Biol. Chem. **275**, 32467-32474
20. Eiserich, J. P., Cross, C. E., Jones, A. D., Halliwell, B. and van der Vliet, A. (1996) Formation of nitrating and chlorinating species by reaction of nitrite with hypochlorous acid. A novel mechanism for nitric oxide-mediated protein modification. J. Biol. Chem. **271**, 19199-19208
21. Zimmerman, M. C., Oberley, L. W. and Flanagan, S. W. (2007) Mutant SOD1-induced neuronal toxicity is mediated by increased mitochondrial superoxide levels. J. Neurochem. **102**, 609-618
22. Ba, X., Gupta, S., Davidson, M. and Garg, N. J. (2010) Trypanosoma cruzi induces the reactive oxygen species-PARP-1-RelA pathway for up-regulation of cytokine expression in cardiomyocytes. J. Biol. Chem. **285**, 11596-11606
23. Lee, S. H., Heo, J. S., Lee, M. Y. and Han, H. J. (2008) Effect of dihydrotestosterone on hydrogen peroxide-induced apoptosis of mouse embryonic stem cells. J. Cell Physiol. **216**, 269-275
24. Mok, J. S., Paisley, K. and Martin, W. (1998) Inhibition of nitrergic neurotransmission in the bovine retractor penis muscle by an oxidant stress: effects of superoxide dismutase mimetics. Br. J. Pharmacol. **124**, 111-118
25. Balaban, R. S., Nemoto, S. and Finkel, T. (2005) Mitochondria, oxidants, and aging. Cell **120**, 483-495
26. Li, N., Ragheb, K., Lawler, G., Sturgis, J., Rajwa, B., Melendez, J. A. and Robinson, J. P. (2003) Mitochondrial complex I inhibitor rotenone induces apoptosis through enhancing mitochondrial reactive oxygen species production. J. Biol. Chem. **278**, 8516-8525
27. Yu, J. H., Kim, C. S., Yoo, D. G., Song, Y. J., Joo, H. K., Kang, G., Jo, J. Y., Park, J. B., Jeon, B. H. (2006) NADPH oxidase and mitochondrial ROS are involved in the TNF-α-induced vascular cell adhesion molecule-1 and monocyte adhesion in cultured endothelial cells. Korean J. Physiol. Pharmacol. **10**, 217-222

28. Sumimoto, H. (2008) Structure, regulation and evolution of Nox-family NADPH oxidases that produce reactive oxygen species. FEBS J. **275**, 3249-3277
29. Squadrito, G. L. and Pryor, W. A. (1998) Oxidative chemistry of nitric oxide: the roles of superoxide, peroxynitrite, and carbon dioxide. Free Radic. Biol. Med. **25**, 392-403
30. Lymar, S. V. and Hurst, J. K. (1996) Carbon dioxide: physiological catalyst for peroxynitrite-mediated cellular damage or cellular protectant? Chem Res Toxicol **9**, 845-850
31. Stanbury, D. M. (1989) Reduction potentials involving inorganic free radicals in aqueous solution. Adv. Inorg. Chem. **33**, 69-138
32. Wardman, P. (1989) Reduction potentials of one-electron couples involving free radicals in aqueous solution. J. Phys. Chem. Ref. Data **18**, 1637-1755
33. Huie, R. E., Clifton, C. L. and Neta, P. (1991) Electron transfer reaction rates and equilibria of the carbonate and sulfate radical anions. Radiat. Phys. Chem. **38**, 477-481
34. Steenken, S. and Jovanovic, S. (1997) How easily oxidizable is DNA? One-electron reduction potentials of adenosine and guanosine radicals in aqueous solution. J. Am. Chem. Soc. **119**, 617-618
35. Burner, U., Furtmuller, P. G., Kettle, A. J., Koppenol, W. H. and Obinger, C. (2000) Mechanism of reaction of myeloperoxidase with nitrite. J. Biol. Chem. **275**, 20597-20601
36. Furtmuller, P. G., Arnhold, J., Jantschko, W., Pichler, H. and Obinger, C. (2003) Redox properties of the couples compound I/compound II and compound II/native enzyme of human myeloperoxidase. Biochem. Biophys. Res. Commun. **301**, 551-557
37. Jantschko, W., Furtmuller, P. G., Allegra, M., Livrea, M. A., Jakopitsch, C., Regelsberger, G. and Obinger, C. (2002) Redox intermediates of plant and mammalian peroxidases: a comparative transient-kinetic study of their reactivity toward indole derivatives. Arch. Biochem. Biophys. **398**, 12-22
38. Strader, C. D., Fong, T. M., Tota, M. R., Underwood, D. and Dixon, R. A. (1994) Structure and function of G protein-coupled receptors. Annu. Rev. Biochem. **63**, 101-132
39. Kang, K. W., Choi, S. H. and Kim, S. G. (2002) Peroxynitrite activates NF-E2-related factor 2/antioxidant response element through the pathway of phosphatidylinositol 3-kinase: the role of nitric oxide synthase in rat glutathione S-transferase A2 induction. Nitric Oxide **7**, 244-253
40. Park, J., Lee, J. and Choi, C. (2011) Mitochondrial network determines intracellular ROS dynamics and sensitivity to oxidative stress through switching inter-mitochondrial messengers. PLoS One **6**, e23211
41. Zhang, F., Jin, S., Yi, F., Xia, M., Dewey, W. L. and Li, P. L. (2008) Local production of O2- by NAD(P)H oxidase in the sarcoplasmic reticulum of coronary arterial myocytes: cADPR-mediated Ca2+ regulation. Cell. Signal. **20**, 637-644
42. Tokutomi, Y., Kataoka, K., Yamamoto, E., Nakamura, T., Fukuda, M., Nako, H., Toyama, K., Dong, Y. F., Ahmed, K. A., Sawa, T., Akaike, T. and Kim-Mitsuyama, S. (2011) Vascular responses to 8-nitro-cyclic GMP in non-diabetic and diabetic mice. Br. J. Pharmacol. **162**, 1884-1893

FIGURE LEGENDS

FIGURE 1. **$ONOO^-$-dependent nitration of guanine nucleotides and tyrosine**
(**A**) Nitration of various guanine nucleotides by $ONOO^-$. The guanine nucleotides cGMP, GMP, GDP, and GTP (1 mM each) were reacted with 2 mM $ONOO^-$ in 0.1 M sodium phosphate buffer (pH 7.4) in the presence of 25 mM $NaHCO_3$. (**B**) Nitration of cGMP (left panel) and tyrosine (right panel) by $ONOO^-$ as a function of $ONOO^-$ concentration. (**C**) pH dependence of $ONOO^-$-mediated nitration of cGMP and tyrosine. In *B* and *C*, cGMP (50 μM) or tyrosine (50 μM) was reacted with the indicated concentration of $ONOO^-$ and different pH range, respectively. Data are expressed as means ± S.E. (n = 3). * $p < 0.05$ and ** $p < 0.01$, compared with the group in the absence of $NaHCO_3$.

FIGURE 2. **Effects of ROS scavengers on formation of 8-nitro-cGMP induced by various RNOS systems**
cGMP (50 μM) was reacted with authentic $ONOO^-$ (5 μM) (**A**), with SIN-1 (100 μM) (**B**), or with $NaNO_2$ (100 μM)/H_2O_2 (100 μM)/MPO (10 nM) (**C**) in the absence or presence of SOD (10 and 100 U/ml), catalase (100 and 1000 U/ml), or tiron (20 and 200 μM). Data are expressed as means ± S.E. (n = 3). * $p < 0.05$ and ** $p < 0.01$ compared with control.

FIGURE 3. **Immunocytochemical analysis of 8-nitro-cGMP formation in rat C6 glioma cells and modulation of its formation by ROS scavengers**
Cells were stimulated with a mixture of LPS (10 μg/ml), IFN-γ (200 U/ml), TNFα (500 U/ml), and IL-1β (10 ng/ml) for 36 h in the absence or presence of the indicated concentrations of PEG-SOD or PEG-catalase. Cells were then fixed with Zamboni fixative as described under "Experimental Procedures," followed by immunocytochemical detection of intracellular 8-nitro-cGMP with the use of 1G6 monoclonal antibody against 8-nitro-cGMP. (**A**) cells were treated with different concentrations of PEG-SOD (upper panels) or PEG-catalase (lower panels) (from 1 h before addition of LPS-cytokines), during stimulation with LPS-cytokines for 36 h, followed by immunocytochemical detection of 8-nitro-cGMP. Scale bars indicate 50 μm. (**B**) Concentration-dependent decrease in relative fluorescence intensity of 8-nitro-cGMP in C6 cells after addition of the cell-permeable superoxide scavenger PEG-SOD (1-200 U/ml) during stimulation with LPS-cytokines. (**C**) Concentration-dependent decrease in relative fluorescence intensity of 8-nitro-cGMP in C6 cells after addition of the cell-permeable H_2O_2 scavenger PEG-catalase (1-200 U/ml) during stimulation with LPS-cytokines. Data are expressed as means ± S.E. (n = 3). **, $p < 0.01$, compared with the LPS-cytokine-treated group.

FIGURE 4. **LC-ESI-MS/MS analysis of 8-nitro-cGMP formation in rat C6 glioma cells and modulation of its formation by ROS scavengers**
Cells were stimulated with a mixture of LPS (10 μg/ml), IFN-γ (200 U/ml), TNFα (500 U/ml), and IL-1β (10 ng/ml) for 36 h in the absence or presence of PEG-SOD or PEG-catalase, and cell extracts were prepared as described under "Experimental Procedures," followed by LC-ESI-MS/MS

quantification of cGMP and 8-nitro-cGMP formed in cells. (**A**) LC-ESI-MS/MS chromatograms of cGMP and 8-nitro-cGMP in untreated cells and cells treated with 200 U/ml PEG-SOD or 200 U/ml PEG-catalase (from 1 h before LPS-cytokine addition), during stimulation with LPS-cytokines for 36 h. (**B**) Intracellular cGMP concentrations in cells after stimulation with LPS-cytokines in the presence or absence of PEG-SOD or PEG-catalase (each at 200 U/ml) determined with LC-ESI-MS/MS. (**C**) Intracellular 8-nitro-cGMP concentrations in cells after stimulation with LPS-cytokines in the presence or absence of PEG-SOD or PEG-catalase (each at 200 U/ml) determined with LC-ESI-MS/MS. Data are expressed as means ± S.E. ($n = 3$). *, $p < 0.05$ and **, $p < 0.01$ compared with the LPS-cytokines-treated group. ##, $p < 0.01$, compared with the PBS-treated group.

FIGURE 5. **Fluorescence microscopic determination of ROS production in rat C6 glioma cells stimulated with LPS-cytokines**

Cells were stimulated with a mixture of LPS (10 μg/ml), IFN-γ (200 U/ml), TNFα (500 U/ml), and IL-1β (10 ng/ml) for 36 h in the absence or presence of PEG-SOD or PEG-catalase. Cells were then analyzed for the presence of mitochondrial superoxide and cellular H_2O_2, as described under "Experimental Procedures." (**A**) MitoSOX Red (upper panels), DCDHF-DA (middle panels), and DHE (lower panels) staining of untreated cells and cells treated with 200 U/ml PEG-SOD or 200 U/ml PEG-catalase (from 1 h before LPS-cytokine addition), during stimulation with LPS-cytokines for 36 h, as detected by the Nikon EZ-C1 confocal laser microscope (for MitoSOX Red: excitation at 420 nm and red photomultiplier channel; for DCDHF-DA: excitation at 488 nm and green photomultiplier channel; and for DHE: excitation at 543 nm and red photomultiplier channel). Scale bars indicate 50 μm. (**B**) Relative fluorescence intensity for MitoSOX Red staining (upper panel), DCDHF-DA staining (middle panel), and DHE staining (lower panel) of untreated C6 cells or cells treated with 200 U/ml PEG-SOD or 200 U/ml PEG-catalase (from 1 h before LPS-cytokine addition), during stimulation with LPS-cytokines for 36 h. Data are expressed as means ± S.E. ($n = 3$). **, $p < 0.01$, compared with the LPS-cytokine-treated group.

FIGURE 6. **Effect of the SOD mimic tiron on formation of 8-nitro-cGMP and ROS production in rat C6 glioma cells**

Cells were stimulated with a mixture of LPS (10 μg/ml), IFN-γ (200 U/ml), TNFα (500 U/ml), and IL-1β (10 ng/ml) for 36 h in the absence or presence of tiron (1-100 μM), followed by immunocytochemical detection of intracellular 8-nitro-cGMP with the use of 1G6 monoclonal antibody against 8-nitro-cGMP, or by direct staining for mitochondrial superoxide or cellular H_2O_2 as described under "Experimental Procedures." Cells were untreated or treated with 1-100 μM tiron (from 1 h before LPS-cytokine addition), during stimulation with LPS-cytokines for 36 h, followed by immunocytochemical detection of 8-nitro-cGMP (**A**, upper panels); detection of MitoSOX Red staining (**A**, middle panels), via a Nikon EZ-C1 confocal laser microscope (excitation, 420 nm; red photomultiplier channel); and detection of DCDHF-DA staining (**A**, lower panels), via a Nikon EZ-C1 confocal laser microscope (excitation, 488 nm; green photomultiplier channel). Scale bars indicate 50 μm. (**B**) Relative fluorescence intensity of C6 cells, treated as described above, for 8-nitro-cGMP

immunocytochemical staining (left panel), MitoSOX Red staining (middle panel), and DCDHF-DA staining (right panel). Data are expressed as means ± S.E. (n = 3). **, $p < 0.01$, compared with the LPS-cytokine-treated group.

FIGURE 7. **Modulation of 8-nitro-cGMP formation by rotenone in rat C6 glioma cells**
Cells were stimulated with a mixture of LPS (10 μg/ml), IFN-γ (200 U/ml), TNFα (500 U/ml), and IL-1β (10 ng/ml) for 36 h in the absence or presence of rotenone (10 μM). Cells were then fixed with Zamboni fixative as described under "Experimental Procedures," followed by immunocytochemical detection of intracellular 8-nitro-cGMP with the use of 1G6 monoclonal antibody against 8-nitro-cGMP, or by direct staining for mitochondrial superoxide or cellular H_2O_2. Cells were pretreated with 10 μM rotenone (from 15 min before LPS-cytokine addition) or were untreated, during stimulation with LPS-cytokines for 36 h, followed by immunocytochemical detection via a Nikon EZ-C1 confocal laser microscope of 8-nitro-cGMP (**A**, upper panels); MitoSOX Red staining (excitation, 420 nm; red photomultiplier channel) (**A**, upper middle panels); DCDHF-DA staining (excitation, 488 nm; green photomultiplier channel) (**A**, lower middle panels), and DHE staining (excitation, 543 nm; red photomultiplier channel) (**A**, lower panels). Scale bars indicate 50 μm. (**B**) relative fluorescence intensity of C6 cells, treated as just described, for 8-nitro-cGMP immunocytochemical staining (upper left panel); MitoSOX Red staining (lower left panel); DCDHF-DA staining (upper right panel); and DHE staining (lower right panel). *C,* intracellular 8-nitro-cGMP concentrations in cells after stimulation with LPS-cytokines with or without 10 μM rotenone pretreatment, as determined with LC-ESI-MS/MS. Data are expressed as means ± S.E. (n = 3). **, $p < 0.01$, compared with the LPS-cytokine-treated group. ##, $p < 0.01$ compared with PBS-treated gourp.

FIGURE 8. **Effects of Nox2 gene knockdown on formation of 8-nitro-cGMP and ROS production rat C6 glioma cells**
Cells were transfected with control siRNA or $p47^{phox}$-specific siRNA as described under "Experimental Procedures," followed by stimulation with a mixture of LPS (10 μg/ml), IFN-γ (200 U/ml), TNFα (500 U/ml), and IL-1β (10 ng/ml) for 36 h. Immunocytochemistry with 1G6 monoclonal antibody against 8-nitro-cGMP was used to detect intracellular 8-nitro-cGMP, or direct staining was used for mitochondrial superoxide or cellular H_2O_2. (**A**) Immunocytochemistry for 8-nitro-cGMP (1G6; upper panels); fluorescent staining of mitochondrial superoxide (MitoSOX Red; middle panels); and fluorescent staining of intracellular H_2O_2 (DCDHF-DA; lower panels). Scale bars indicate 50 μm. (**B**) Relative fluorescence intensity of C6 cells, treated as described above, for 8-nitro-cGMP immunocytochemical staining (upper left panel); MitoSOX Red staining (lower left panel); and DCDHF-DA staining (lower right panel). The upper right panel shows the Western blot for the $p47^{phox}$ knockdown. Data are expressed as means ± S.E. (n = 3). **, $p < 0.01$, compared with the LPS-cytokine plus negative control siRNA-treated group.

FIGURE 9. **Increase in 8-nitro-cGMP formation and mitochondrial superoxide production in rat**

C6 glioma cells by H_2O_2 and NO treatment

(**A**) Cells were untreated or treated with 10 or 100 μM H_2O_2 for 36 h, plus PEG-SOD (200 U/ml), P-NONOate (100 μM), or PEG-SOD (200 U/ml) plus P-NONOate (100 μM). Immunocytochemistry for intracellular 8-nitro-cGMP with the use of 1G6 monoclonal antibody against 8-nitro-cGMP, as described under "Experimental Procedures," followed. Scale bars indicate 50 μm. (**B**) in other experiments, cells were untreated or treated only with 10 or 100 μM H_2O_2, followed by detection of mitochondrial superoxide generation by MitoSOX Red staining as described under "Experimental Procedures," (left panels). Scale bars indicate 50 μm.

FIGURE 10. **Schematic drawing of possible mechanisms involved in cell formation of 8-nitro-cGMP in rat C6 glioma cells stimulated with LPS-cytokines**

Table 1. Nitration of cGMP (50 μM) and tyrosine (50 μM) by various RNOS systems

Conditions	Product formed (nM)	
	8-Nitro-cGMP	3-Nitrotyrosine
NONOate (100 μM), 4 h#	ND†	16.7 ± 1.1 *
$NaNO_2$ (100 μM), at pH 3.0, 1 h‡	ND	95.8 ± 1.8 *
$NaNO_2$ (100 μM), at pH 4.0, 1 h‡	ND	30.3 ± 3.0 *
SIN-1 (50 μM), 2 h§	7.7 ± 0.3 *	267.3 ± 5.6 *
SIN-1 (100 μM), 2 h§	14.5 ± 0.7 *	402.9 ± 8.3 *
$NaNO_2$ (100 μM), H_2O_2 (100 μM), MPO (10 nM), 4 h‖	67.3 ± 1.5 *	8307.0 ± 11.1 *
$NaNO_2$ (100 μM), MPO (10 nM), 4 h‖	ND	ND
H_2O_2 (100 μM), MPO (10 nM), 4 h‖	ND	ND
$NaNO_2$ (100 μM), H_2O_2 (100 μM), 4 h‖	ND	ND
$NaNO_2$ (100 μM), H_2O_2 (100 μM), HRP (23.8 μM), 4 h‖	ND	803.5 ± 1.6 *
HOCl (100 μM), $NaNO_2$ (100 μM), 4 h¶	ND	48.3 ± 1.9 *

#In 0.1 M sodium phosphate buffer (pH 7.4), 0.1 mM DTPA, at 37 °C.
†ND, not detected.
‡In 0.1 M sodium citrate buffer (pH 2.5-4.5) , 100 μM $NaNO_2$, at 37 °C.
§In 0.1 M sodium phosphate buffer (pH 7.4), 0.1 mM DTPA, 25 mM $NaHCO_3$, at 37 °C.
‖In 0.1 M sodium phosphate buffer (pH 7.4), at 37 °C.
¶In 0.1 M citric acid buffer (pH 4.5), at 37 °C.
*, $p < 0.01$, compared with the control (no RNOS treatment).

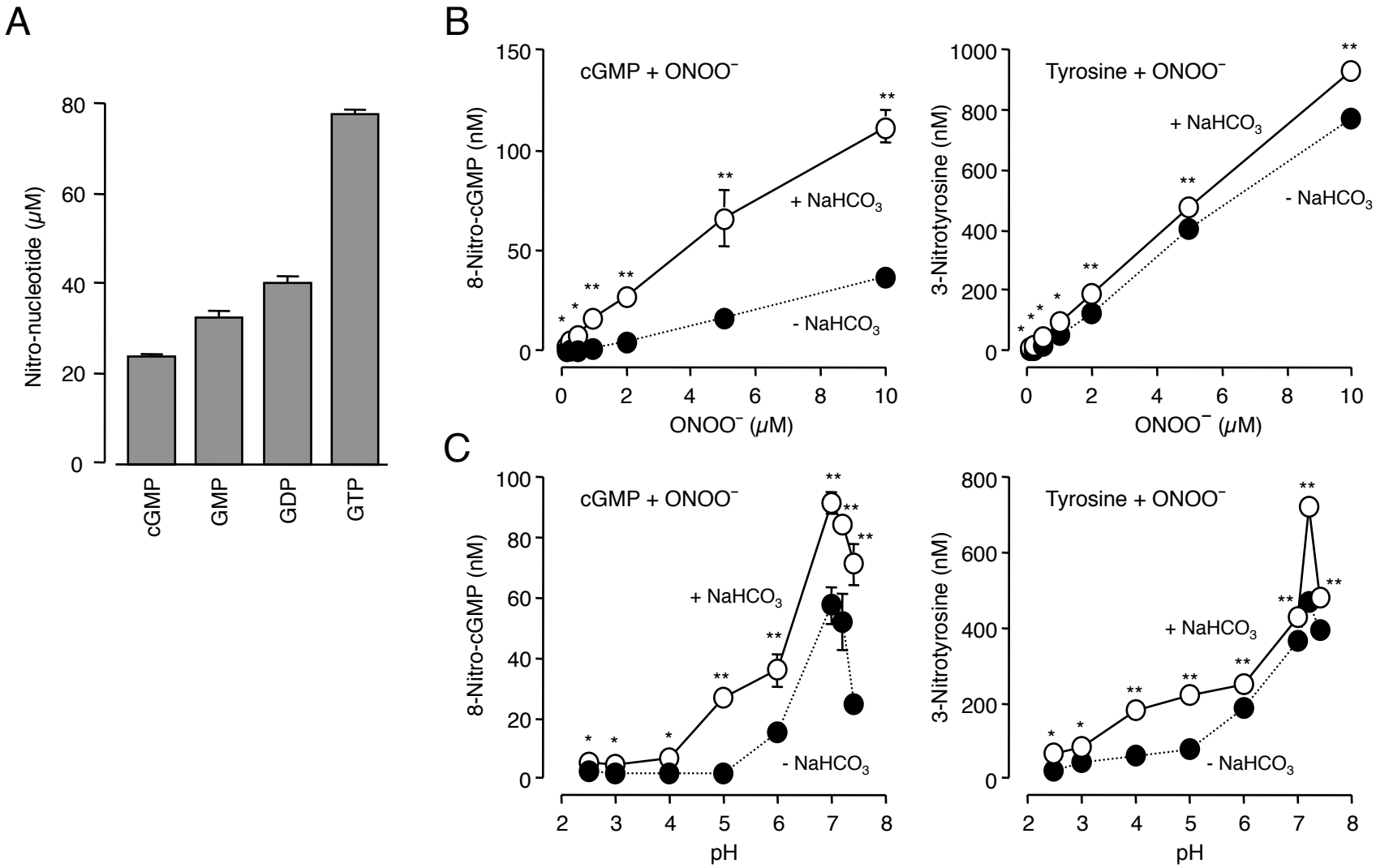
A
Nitro-nucleotide (μM)
0
20
40
60
80
cGMP
GMP
GDP
GTP
B
cGMP + ONOO⁻
8-Nitro-cGMP (nM)
+ NaHCO3
- NaHCO3
ONOO⁻ (μM)
Tyrosine + ONOO⁻
3-Nitrotyrosine (nM)
C
pH

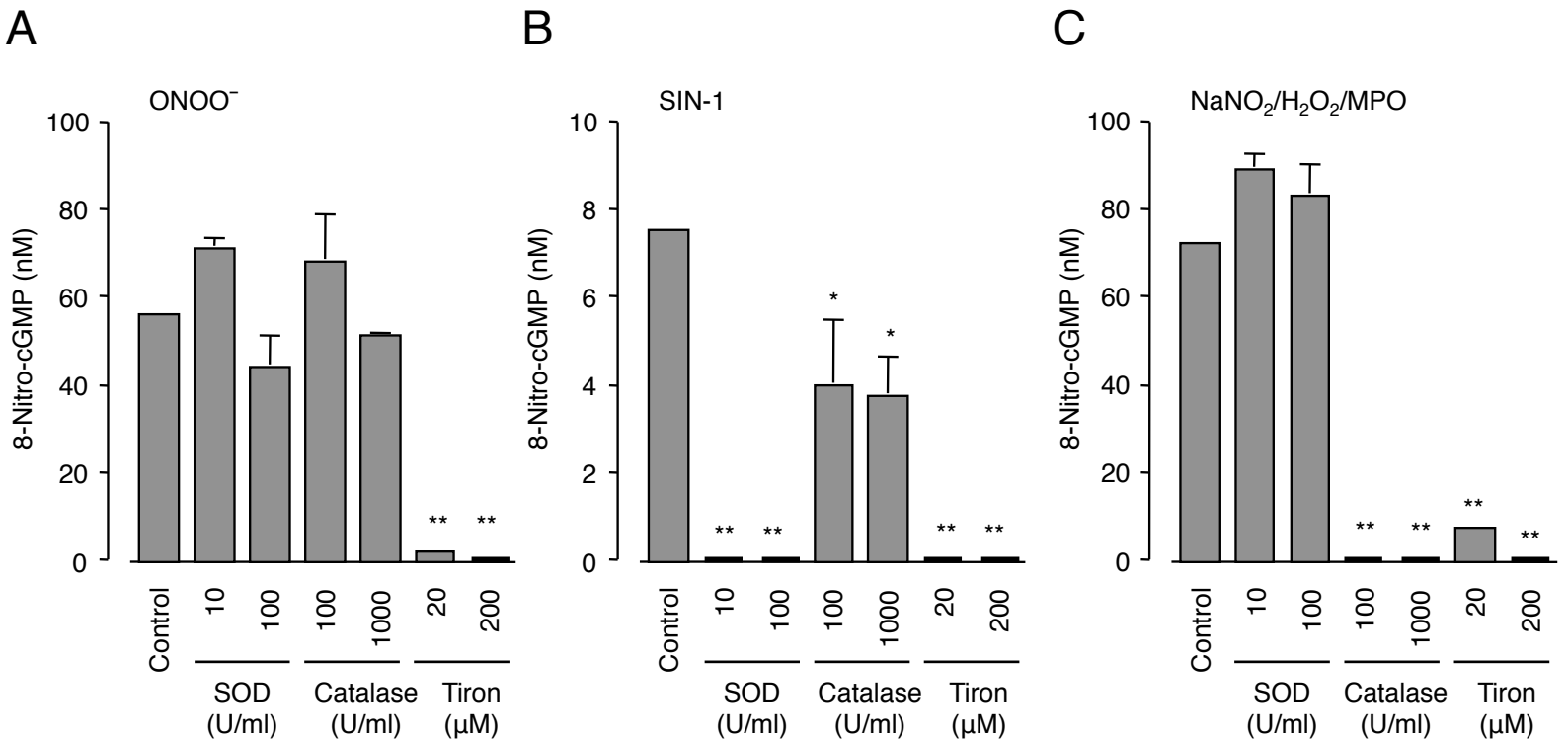
A
ONOO⁻
8-Nitro-cGMP (nM)
100
80
60
40
20
0
**
**
Control
10
100
100
1000
20
200
SOD (U/ml)
Catalase (U/ml)
Tiron (μM)
B
SIN-1
8-Nitro-cGMP (nM)
10
8
6
4
2
0
**
**
*
*
**
**
Control
10
100
100
1000
20
200
SOD (U/ml)
Catalase (U/ml)
Tiron (μM)
C
NaNO2/H2O2/MPO
8-Nitro-cGMP (nM)
100
80
60
40
20
0
**
**
**
**
Control
10
100
100
1000
20
200
SOD (U/ml)
Catalase (U/ml)
Tiron (μM)

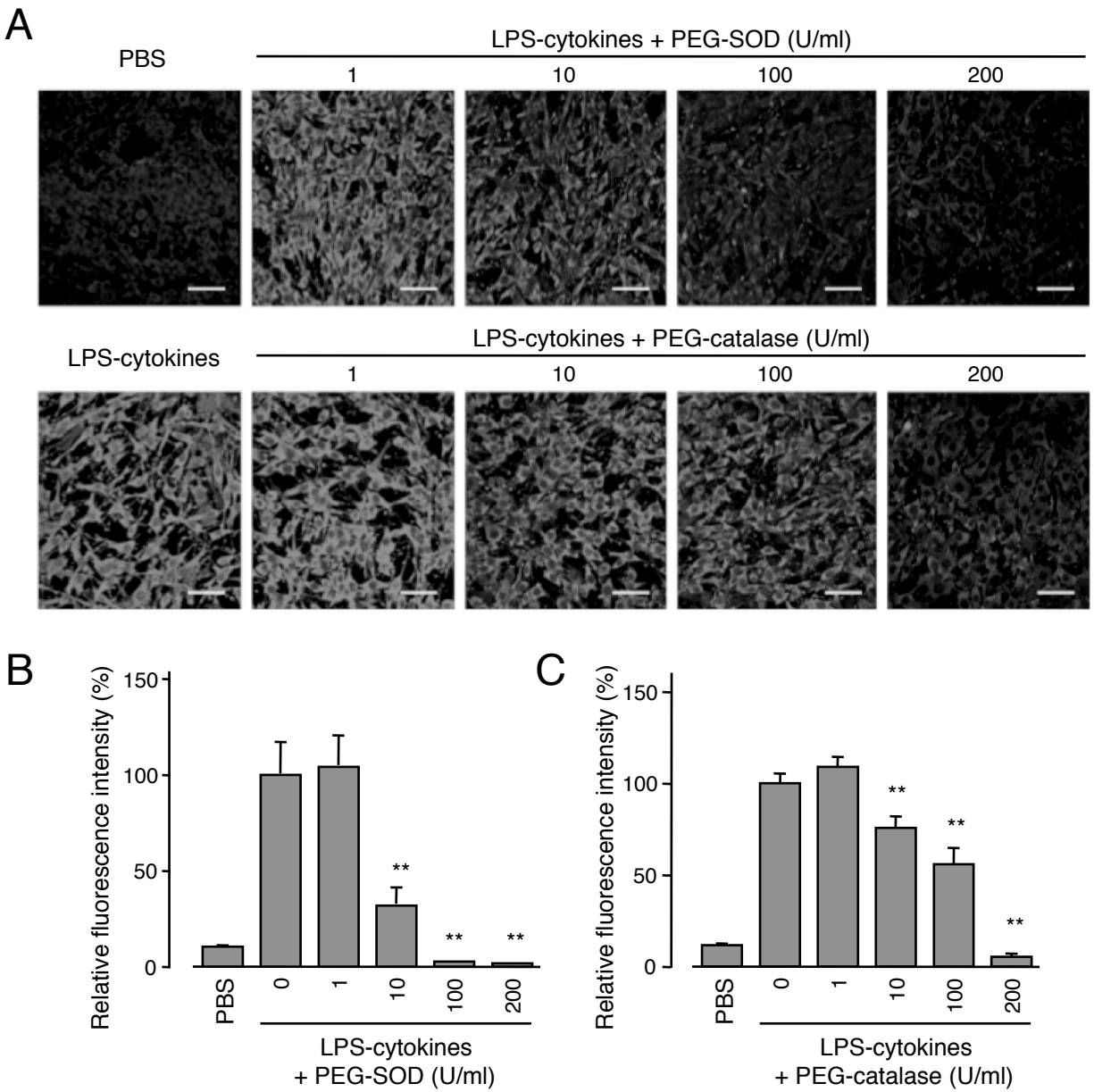
A
PBS
LPS-cytokines + PEG-SOD (U/ml)
1
10
100
200
LPS-cytokines
LPS-cytokines + PEG-catalase (U/ml)
1
10
100
200
B
Relative fluorescence intensity (%)
150
100
50
0
**
**
**
PBS
0
1
10
100
200
LPS-cytokines
+ PEG-SOD (U/ml)
C
Relative fluorescence intensity (%)
150
100
50
0
**
**
**
PBS
0
1
10
100
200
LPS-cytokines
+ PEG-catalase (U/ml)

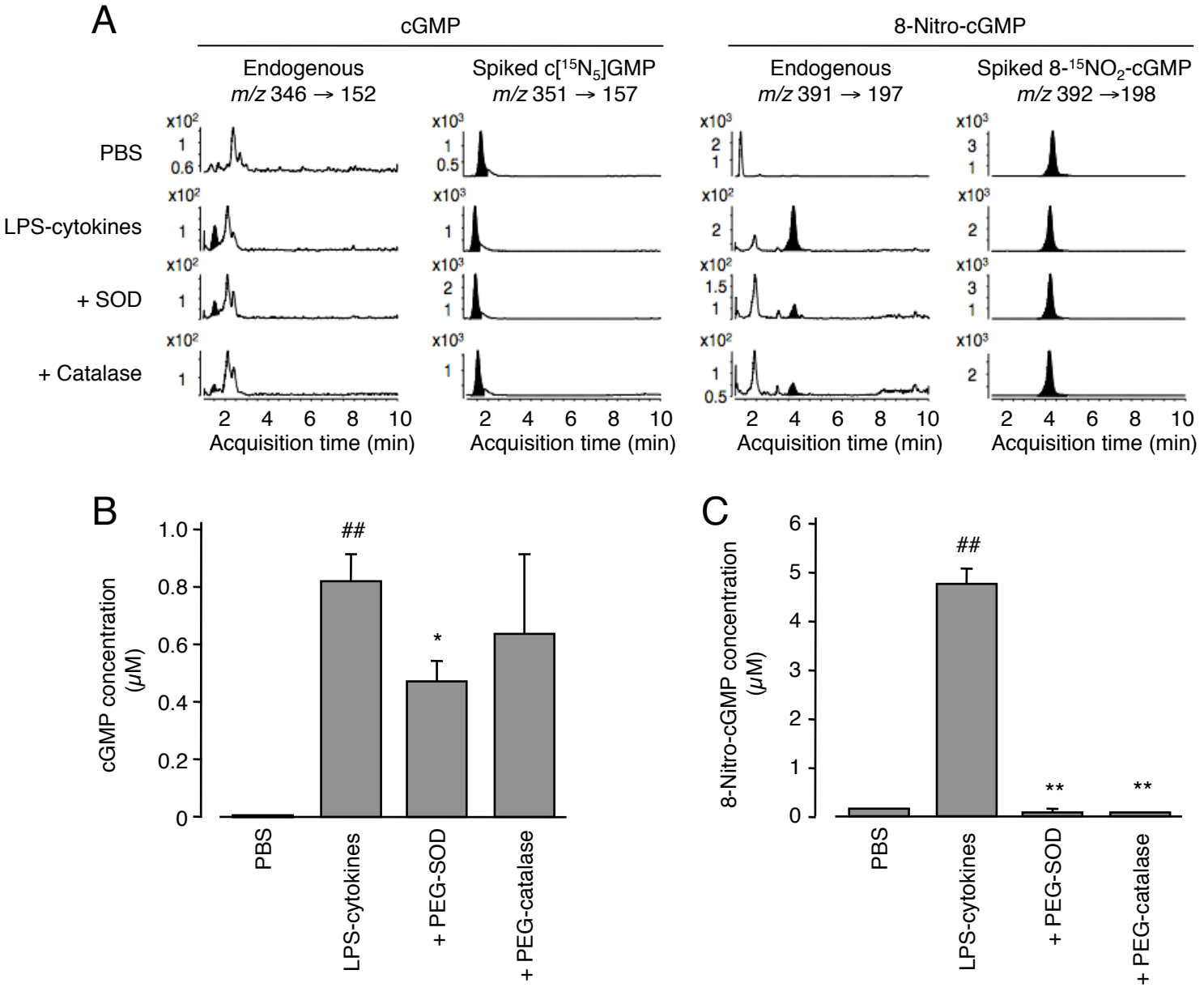
A
cGMP
8-Nitro-cGMP
Endogenous
m/z 346 → 152
Spiked c[15N5]GMP
m/z 351 → 157
Endogenous
m/z 391 → 197
Spiked 8-15NO2-cGMP
m/z 392 →198
PBS
LPS-cytokines
+ SOD
+ Catalase
Acquisition time (min)
B
cGMP concentration (μM)
##
*
PBS
LPS-cytokines
+ PEG-SOD
+ PEG-catalase
C
8-Nitro-cGMP concentration (μM)
##
**
**
PBS
LPS-cytokines
+ PEG-SOD
+ PEG-catalase

Figure 5

Ahtesham et al

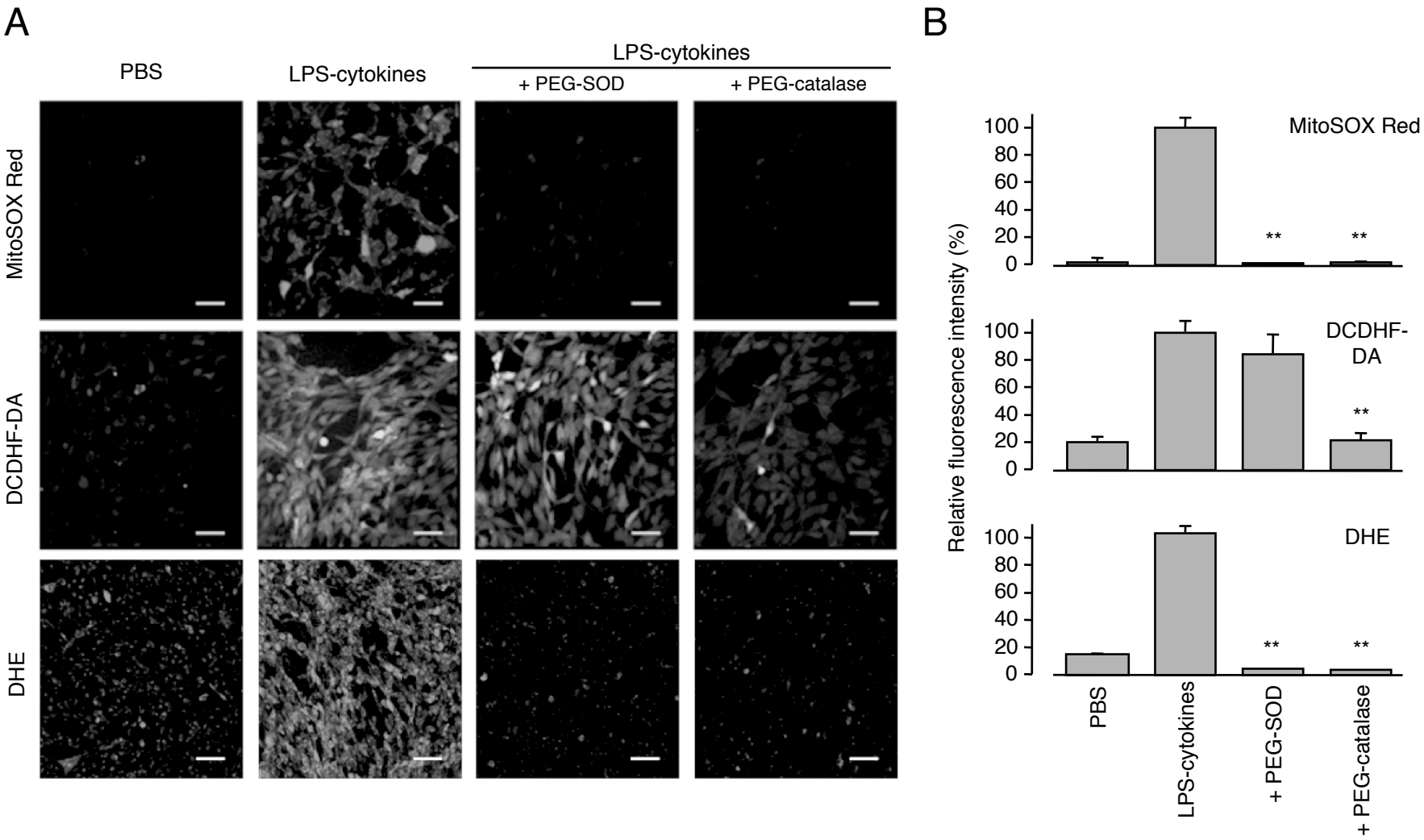

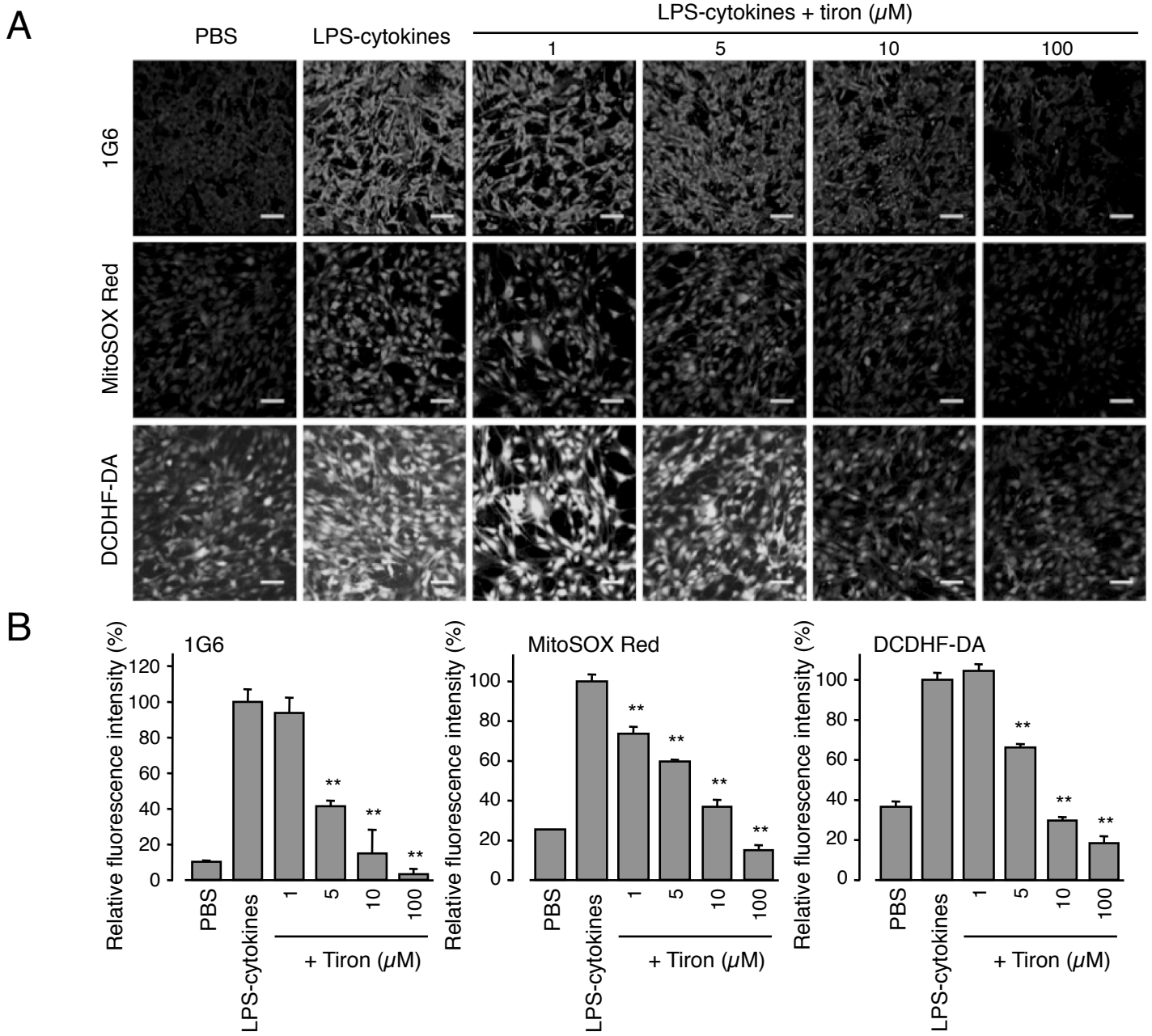
A
PBS
LPS-cytokines
LPS-cytokines + tiron (μM)
1
5
10
100
1G6
MitoSOX Red
DCDHF-DA
B
1G6
MitoSOX Red
DCDHF-DA
Relative fluorescence intensity (%)
PBS
LPS-cytokines
+ Tiron (μM)
**

Figure 7

Ahtesham et al

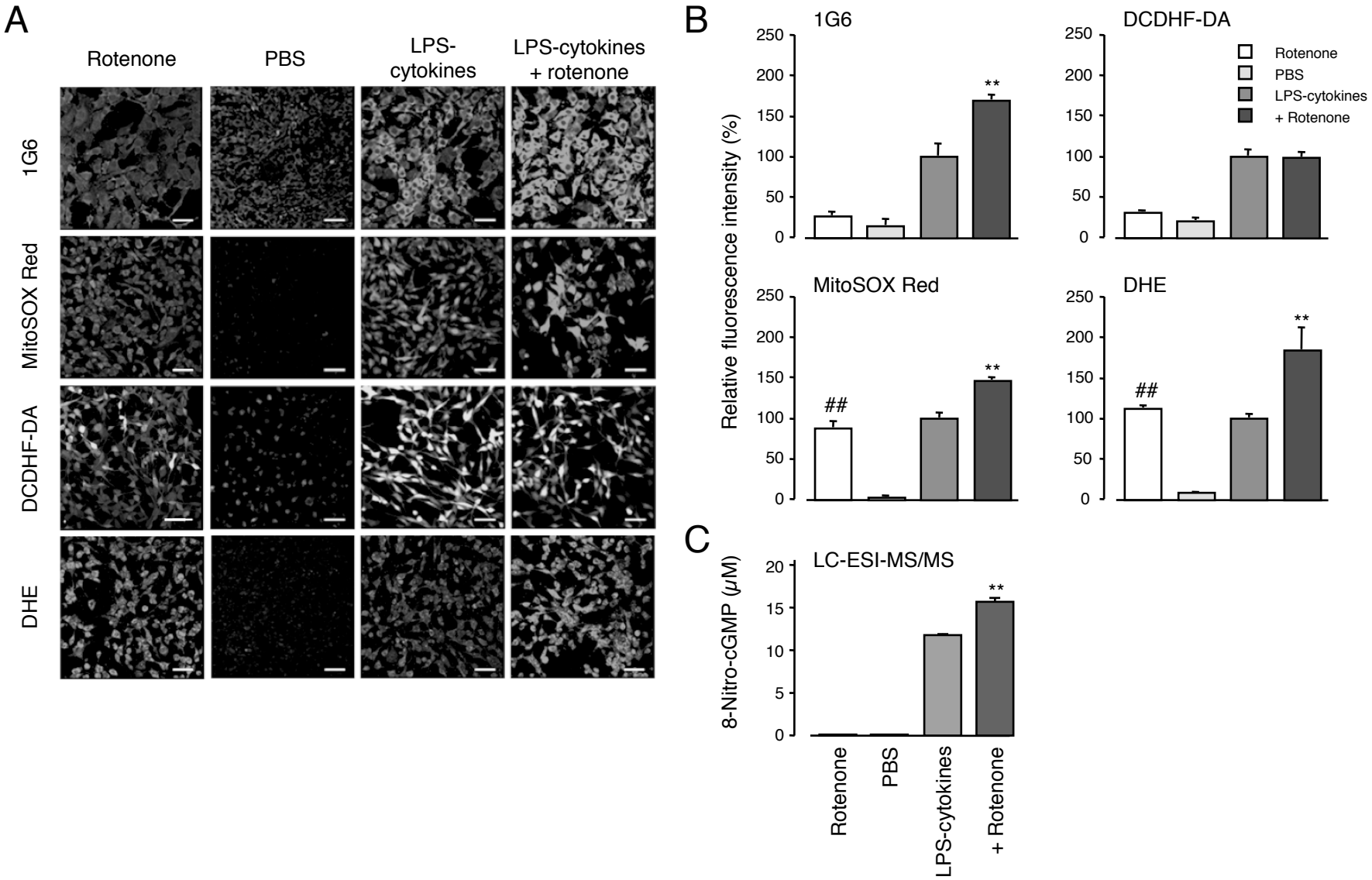

Figure 8

Ahtesham et al

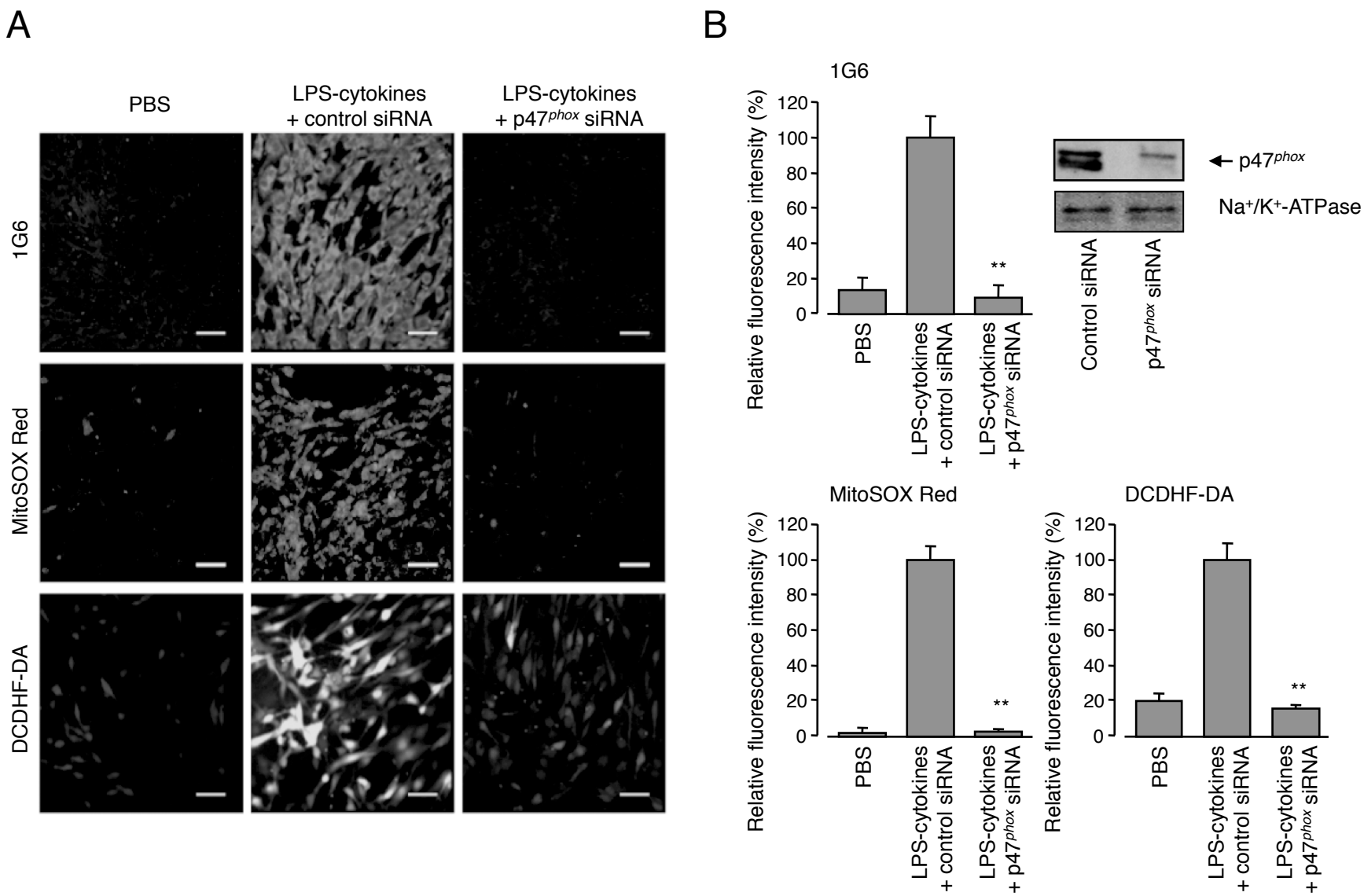

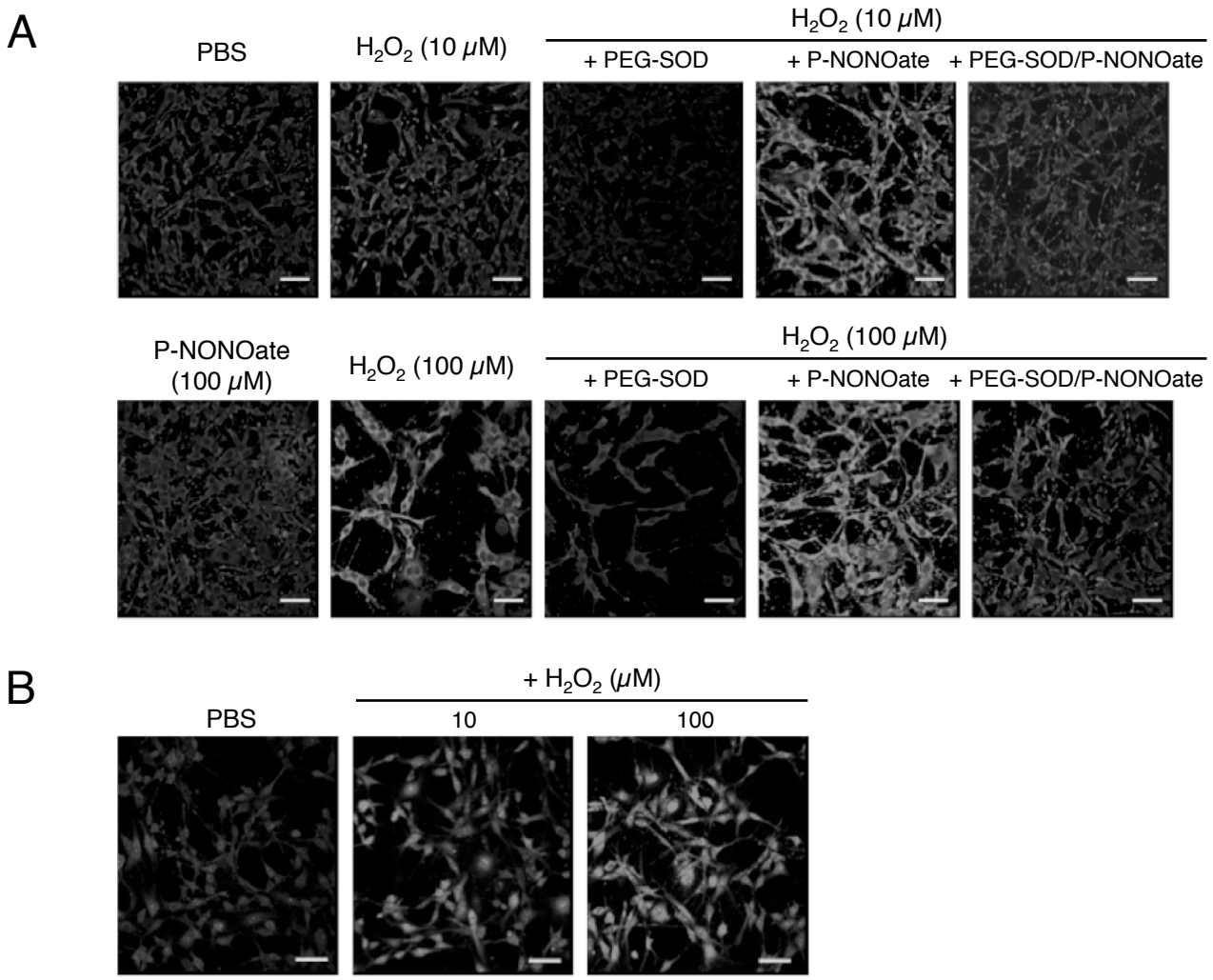
A
PBS
H2O2 (10 μM)
H2O2 (10 μM)
+ PEG-SOD
+ P-NONOate
+ PEG-SOD/P-NONOate
P-NONOate (100 μM)
H2O2 (100 μM)
H2O2 (100 μM)
+ PEG-SOD
+ P-NONOate
+ PEG-SOD/P-NONOate
B
+ H2O2 (μM)
PBS
10
100

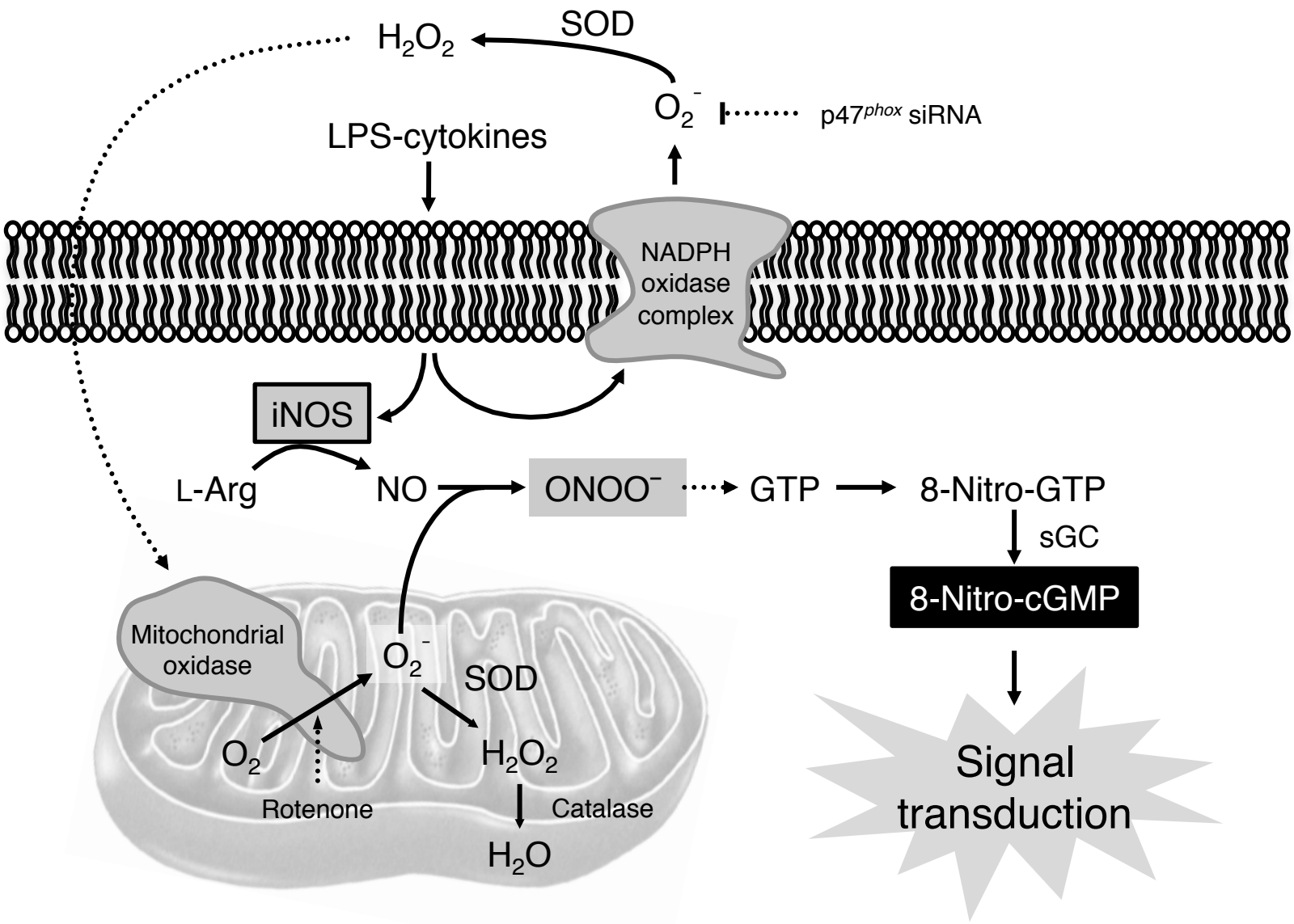
H_2O_2
SOD
O_2^-
p47^{phox} siRNA
LPS-cytokines
NADPH oxidase complex
iNOS
L-Arg
NO
ONOO$^-$
GTP
8-Nitro-GTP
sGC
8-Nitro-cGMP
Mitochondrial oxidase
O_2^-
SOD
O_2
H_2O_2
Rotenone
Catalase
H_2O
Signal transduction